Multi-User Mixed FSO-RF Systems With Aperture Selection Under Poisson Field Interference

IMÈNE TRIGUI[ID][1], **(Member, IEEE), SOFIÈNE AFFES**[ID][1], **(Senior Member, IEEE),**
ANAS M. SALHAB[ID][2], **(Senior Member, IEEE), AND**
MOHAMED-SLIM ALOUINI[ID][3], **(Fellow, IEEE)**
[1]INRS-EMT, Montreal, QC H5A 1K6, Canada
[2]Electrical Engineering Department, King Fahd University of Petroleum and Minerals, Dhahran 31261, Saudi Arabia
[3]Computer, Electrical, and Mathematical Sciences and Engineering Division, King Abdullah University of Science and Technology, Thuwal 23955, Saudi Arabia

Corresponding author: Imène Trigui (itrigui@emt.inrs.ca)

ABSTRACT In this paper, we study the performance of mixed free space optical (FSO)-radio frequency (RF) multi-user relay network with aperture selection and opportunistic user scheduling in the presence of Poisson field interference. The considered system includes multiple optical sources (apertures), one amplify-and-forward (AF) relay, and multiple users. The source is connected with the relay node through FSO links and the relay is connected with the users through RF links with a Poisson field interference at the users. The FSO-RF channels are assumed to follow Málaga-$\mathcal{M}$/shadowed κ-μ fading models with pointing errors on the FSO links. Exact closed-form expressions are derived for the outage probability and average symbol error probability (SEP). Moreover, the system performance is studied at the high signal-to-noise ratio (SNR) regime, where an approximate expression for the system outage probability is derived, in addition to deriving the system diversity order and coding gain. Then, the optimum source and relay transmission powers and relay position are determined to minimize the system asymptotic outage probability. The Monte-Carlo simulations are provided to validate the achieved exact and asymptotic results.

INDEX TERMS Mixed FSO-RF relay network, Málaga-$\mathcal{M}$ distribution, shadowed κ-μ fading, aperture selection, multiuser diversity, Poisson field interference, pointing errors, power allocation.

I. INTRODUCTION

Recently, the scenario of mixed free space optical (FSO)-radio frequency (RF) relaying has been proposed as an efficient solution for current and future wireless networks from different aspects. Such type of mixed networks possesses the features both of licensed-free FSO communications such as high security, flexibility, rapid deployment time, and rigidity to RF interference [1] and of cooperative relay networks such as resilience to multi-path fading in wireless communications [2]. Having relays in wireless networks provides diversity, widens the coverage area, and reduces the need for high-power transmitters. Combining the FSO communications with relay networks aims to increase the coverage distance of FSO networks which is usually limited to a few hundred meters in realistic conditions due to atmospheric turbulence effects [3].

The associate editor coordinating the review of this manuscript and approving it for publication was Taufik Abrao.

Another important application for mixed RF-FSO or FSO-RF relaying scenarios is user multiplexing where multiple users having only RF capability can be multiplexed into a single FSO link [4]. The FSO-RF relay communication has the ability to fill the connectivity gap between the last-mile network and the backbone network as in developing countries by delivering it through high-speed FSO links [6]. Such mixed relaying scheme conserves economic resources by avoiding unnecessary modifications to current mobile devices and at the same time saves bandwidth by utilizing FSO capabilities. These attractive features of mixed FSO-RF relay networks make them a strong candidate for current and soon-to-come wireless networks.

Several studies in the literature considered the scenarios of mixed RF-FSO and FSO-RF relay networks [7]–[52] either with amplify-and-forward (AF) or decode-and-forward (DF) relaying schemes. In the area of AF relaying, the authors in [7] and [8] investigated the performance of an AF mixed RF-FSO relay network over Nakagami-m and

Gamma-Gamma fading channels. Exact closed-form and analytical expressions were, respectively, derived in [7] and [8] for the outage probability, average bit error rate (BER), and channel capacity. Considering the outdated channel-state-information (CSI) effect on the RF link and misalignment error on the FSO link, the authors in [9] evaluated the performance of an AF mixed RF-FSO relay network over Rayleigh and a Gamma-Gamma fading models. The same system model was studied in [10], but with κ-μ and η-μ fading models for the RF link and Gamma-Gamma fading model for the FSO link, whereas it was studied assuming Rayleigh fading for the RF link and Málaga-$\mathcal{M}$ distribution model for the FSO link in [11].

In [12], the authors investigated the performance of an AF mixed RF-FSO relay network while including the direct link between the source and destination. They assumed Nakagami-m fading model for the RF links and a generalized Gamma-Gamma fading model for the FSO link when deriving closed-form expressions for the outage and bit error probabilities. The work on AF mixed RF-FSO relay networks continued in [13] where the authors considered a millimeter-wave (mmWave) Rician distributed RF channel and a Málaga-$\mathcal{M}$ distributed FSO channel. Such mixed scenarios which combine mmWave RF and FSO techniques are preferable in high-density 5G small cells where vast data rates, and hence, very high bandwidths are usually needed. The same system model was also considered in [14], while assuming Weibull and Gamma-Gamma fading models for the mmWave RF and FSO links, respectively. The Weibull distribution is claimed to offer a good fit when modeling the fading amplitude fluctuations in both indoor and outdoor wireless communications [15]. Also, it fits very well for small-scale fading in 5G mmWave communication scenarios [16].

A more general shadowed κ-μ distribution was recently adopted to model the RF links. This model offers an excellent fit to the fading observed in a broad range of real-world applications (e.g. device-to-device and body-centric fading channels [17]). It encompasses several RF channel models such as Nakagami-m, Rayleigh, Rice, κ-μ, and shadowed Rician fading distributions. Also, it offers far better and much more flexible representations of practical fading LOS (line-of-sight), NLOS (non-LOS), and shadowed channels than the Rayleigh and Nakagami-m distributions.

In [18], the authors studied the performance of a mixed FSO-RF relay network assuming Málaga-$\mathcal{M}$/shadowed κ-μ fading models. They derived exact and asymptotic (i.e., high signal-to-noise ratio (SNR) values) closed-form expressions for the system outage probability and channel capacity. The mixed RF-FSO relay network was investigated in [19] from a security point of view and in a cognitive radio scenario in [20]. The performance of a mixed FSO-RF relay network with multiple antennas at the relay node and interference at the RF destination was studied in [21]. Also, an AF mixed RF-FSO relay network with multiple antennas at the source and multiple apertures at the destination was investigated in [22].

In the context of DF relaying, the authors in [23] derived exact closed-form expressions for the outage probability, BER, and channel capacity of a mixed RF-FSO relay network assuming η-μ and Gamma-Gamma fading models. Moreover, the authors in [24] considered the composite κ-μ/Inverse Gaussian fading model to represent the FSO link in a DF mixed RF-FSO relay network. Both the outage probability and error rate performances were studied long with the channel capacity. Trying to improve performance measures, Al-Ebraheemy *et al.* developed in [25] a new expression for the channel capacity which can more accurately represent the channel capacity in the presence of intensity modulation-direct detection (IM/DD) FSO receivers. Based on that result, they derived new unified closed-form expressions for the outage and asymptotic outage probabilities, in addition to deriving the diversity order and coding gain of the system. The performance of DF mixed RF-FSO relay networks with multiple antennas was studied in [26]–[28].

In the area of parallel FSO relaying, the authors in [29] and [30] studied the performance of dual-hop FSO networks over log-normal channels both for the DF and AF schemes, respectively. The performance of a dual-hop FSO selective-relaying network where the source message is forwarded to the destination along the direct link or along the best relay was investigated in [31]. Closed-form and asymptotic expressions were derived for the bit error probability (BEP) assuming Rayleigh and log-normal fading channels. A key paper which provides some new exact and approximate statistics for the sum of Gamma-Gamma variates and their application in RF and FSO DF relay networks was presented in [32]. The outage performance of CSI-assisted and semi-blind AF opportunistic FSO relay networks was studied in [33] assuming composite channels. Considering the effect of outdated channel state estimation of the RF links, the authors in [34] studied the outage and error rate performances of an AF mixed RF-FSO relay network with generalized order relay selection. An optimization problem was formulated in [35] to maximize the throughput of a multiple-relays multiple-destinations AF orthogonal-frequency-division-multiplexing (OFDM) mixed RF-FSO relay network through resource and power allocations for the OFDM subcarriers. A similar optimization problem was formulated in [36] to maximize the throughput of a DF mixed RF-FSO relay network with both conventional and buffer-aided relays. In [37], the author proposed three relaying protocols for the up-link system (RF-FSO) and two schemes for the down-link system (FSO-RF) in an AF mixed RF-FSO relaying network. The protocols have different CSI and symbol selectivity requirements and allow to achieve different levels of compromise between complexity and performance. Most recently, two new papers in the area of mixed RF-FSO relay networks with parallel relaying have appeared in literature, [38] and [39].

The area of mixed RF-FSO relay networks with multiple users has been considered by several researchers in the last few years. In [40], Miridakis *et al.* studied the outage and error probability performances of a multiuser dual-hop

DF mixed RF-FSO relay network with the V-BLAST technique. A resource allocation scheme for a multiuser mixed RF-FSO relay network was proposed in [41], where the data of users on the RF hop are generated according to a zero-mean rotationally invariant complex Gaussian distribution. The authors claimed the effectiveness of the proposed link allocation protocol even when the FSO link is affected by severe atmospheric conditions.

The area of hybrid RF-FSO networks has been recently of interest for many researchers. In [42], considering the cases with and without hybrid automatic repeat request (HARQ) and joint transmission/reception of the RF and FSO messages, the authors derived closed-form expressions for the message decoding probabilities, throughput, and outage probability of the RF-FSO setups. The same scenario was also studied by the same authors in [43], considering, however, the effect of adaptive power allocation on both the system throughput and outage probability. In [44], the outage probability, BER, and channel capacity of a mixed FSO-RF relay network with multiple users were derived both for fixed and CSI-assisted AF relaying schemes.

The performance of multiuser mixed RF-FSO relay networks with outdated channel information and power allocation has been presented in [45], [46]. Opportunistic scheduling where the user of the best RF channel is selected to send its message to the relay node was adopted there. Closed-form expressions for the outage and symbol error probabilities were derived along with the channel capacity taking into account the effect of outdate channel information. In [47], the security of multiuser mixed RF-FSO relay networks was analyzed. The paper studied the effect of a single passive eavesdropper attack on the performance of mixed RF-FSO relay network with multiple users and a multiple-antennas relay. The RF links and FSO link were assumed to follow Nakagami-*m* and Gamma-Gamma fading models, respectively while accounting for the effect of pointing errors on the FSO link. The authors derived closed-form expressions for the outage probability, average symbol error probability (SEP), and channel capacity as reliability performance measures for the authorized mixed RF-FSO relay network and closed-from expression for the intercept probability as a security measure. Asymptotic expressions were also derived for the outage probability at high SNR values and used for achieving the optimum transmission powers of the selected user and relay node. opportunistic scheduling was adopted there to make best selection among users on the first hop. The same authors studied in [48] the effect of RF co-channel interference on the security-reliability tradeoff analysis for DF mixed RF-FSO relay network with single-antenna RF nodes. They formulated and solved a power allocation problem to enhance the overall system performance. Also, they proposed a new cooperative jamming scheme to enhance the security performance of the considered system.

Another study on the effect of interference on the performance of an AF mixed FSO-RF relay network with multiple users is the one presented in [49]. Multiple apertures were assumed at the FSO source and multiple RF users with interference at the RF side. Transmit selection was used at the relay node to select among the FSO signals and opportunistic user scheduling was used at the RF side to select among the RF users. The authors derived closed-form expression for the system capacity following the moment-generating-function (MGF) approach in the analysis. Similar to the system studied in [45], the authors in [50] investigated the performance of an AF mixed RF-FSO relay network with multiple RF users. In the analysis, η-μ fading model was used to model the RF links and $\mathcal{M}$-distribution to model the FSO link. Closed-form expressions were derived for the outage probability, BER, and channel capacity. Aiming at increasing the spectral efficiency, Al-Eryani *et al.* proposed in [51] a new two-way-based relaying scheme for a DF mixed RF-FSO relay network with multiple RF users. They derived closed-form expressions for the outage probability, average symbol error rate, and channel capacity. Compared to one-way relaying protocols, two-way relaying has the ability to almost double the spectral efficient with the same outage performance. The same authors proposed in [52] efficient protocols for buffer-aided DF mixed RF-FSO relay networks with multiple users, multiple antennas relay, and a hybrid RF-FSO second hop. Having buffers at the relay node enables it to receive information for a fixed number of time slots before retransmitting it to destination. This adds some kind of time diversity to the communication system, and hence, enhances its performance at the cost of increased average packet delay.

Most of previous studies considered the scenario of a dual-hop mixed RF-FSO relay network. This scenario could be met in applications in which multiple users communicate with a relay node through RF links and then the relay forwards their massages to a base station (BS) over an FSO link. Also, such a scenario can be encountered in indoor applications where multiple users communicate with an access point that is in turn connected to a macro BS via a FSO link [41]. Besides, it is quite common in practice to see on network downlinks a BS communicate with a relay node over a FSO link and the relay communicates with multiple users over RF links.

Obviously, accounting for the RF interference that is inherent to wireless networks and assessing its impact on the system performance is of noticeable importance. furthermore, combining mmWave and FSO wireless access technologies possesses the key features and advantages of both techniques such as ultra-high data rate transmissions.

In this paper, we investigate the performance of a mixed FSO-RF relay network with multiple RF users and interference on the RF side. The considered system includes an optical source or BS, an AF relay node, and K RF destinations or users. The source is connected with the relay node through an FSO link and the relay is connected with the users through RF links. Each RF user is subject to inter-cell interference brought by Poisson point process (PPP) distributed co-channel RF sources in the network. The system is also extended to include multiple apertures (L) at the BS where

the best received signal among them is selected at the relay node. The FSO link and the RF links are assumed to follow a Málaga-$\mathcal{M}$ and a shadowed κ-μ model, respectively. fading model. The adopted RF fading model is able to represent the mmWave links as a special case. Using opportunistic scheduling, the user with the best SNR among available ones is selected to receive the signal from the relay node. Closed-form expressions are derived for the outage probability and the average SEP. Moreover, the system performance is studied at the high SNR regime, where approximate expressions for the outage probability, diversity order, and coding gain are derived and analyzed. Furthermore, the asymptotic results are exploited to obtain the optimum transmission powers of the BS and the relay node as well as the optimum relay position. Simulation and numerical examples are provided to assess the impact of the number of users, interference, the number of apertures, the atmospheric turbulence parameters, the RF fading parameters, and the power allocation scheme on the system performance.
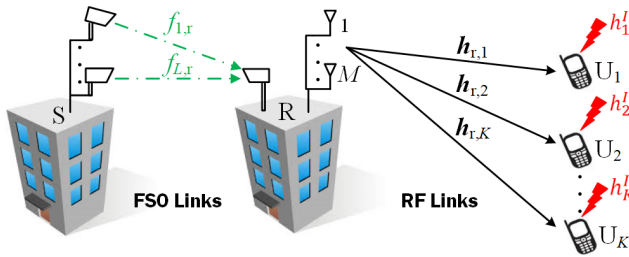

FIGURE 1. Dual-hop mmWave multiuser mixed FSO-RF relay network with opportunistic user scheduling.

II. SYSTEM AND CHANNEL MODELS

As shown in Figure 1, we consider a dual-hop mixed FSO-RF multiuser relay network comprising an optical source (S), an AF relay node (R), and K RF users U_k ($k = 1, \ldots, K$). The source BS is assumed to have L photo-apertures, whereas the relay node R is assumed to have a single photo detector from one side and multiple antennas from the other side, and each user is assumed to be equipped with a single antenna. The BS communicates with the users U_k via an AF relay R with no direct links between them. The communication between the BS and the relay is done over a FSO link, whereas the relay communicates with the users U_k over RF links. Among L apertures at the source, a single aperture that maximizes the pre-processing SNR is selected and used for transmission. The l-th FSO link irradiance is assumed to follow a Málaga-$\mathcal{M}$ distribution with pointing errors impairments. The relay is able to activate either heterodyne or IM/DD detection techniques at the reception of the optical beam. Using AF relaying,[1] all the M transmit antennas at the relay are used for MRT (maximum ratio transmission), while a single user that maximizes the postprocessing SNR is

---

[1]In contrast to a DF relay, an AF relay requires less processing power and complexity. The AF relaying scheme has been widely adopted in the literature on evaluating the performance of mixed FSO/RF relay networks [7]–[14], [18]–[22].

selected for reception. Such a system can multiplex multiple users with RF capability into a single high speed FSO link and then achieve a higher system capacity, thereby providing an adaptive and effective communication system in real communication environments namely cellular downlink and indoor applications [22], [42], [50].

In the meantime, adjacent sources may generate co-channel interference to U_ks, which is of primary focus of our work. The channel gains between the j-th transmit antenna at the relay and the k-th user are denoted by $h_{j,k}$ for $j = 1, 2, \ldots, M$ and $k = 1, 2, \ldots, K$, and are assumed to be independent identically-distributed (i.i.d.) shadowed κ-μ random variables (rvs) over the M antennas at the relay with fading parameters m_k, κ_k, μ_k, and mean $\Omega_k = \mathbb{E}\{h_{j,k}\}$, $k = 1, 2, \ldots, K$, where $\mathbb{E}\{\cdot\}$ denotes the expectation operator. Henceforth, we use the shorthand notation $Z \sim \mathcal{S}(m, \kappa, \mu)$ to denote that the RV Z follows a shadowed κ-μ distribution with parameters m, κ, and μ. The physical parameters κ and μ describe small scale variations in the LOS communication, where μ specifies multi-path clustering and κ denotes the ratio between total power of the dominant components, which are subject to Nakagami-m distribution, and the total power of the scattered waves. The shadowed κ-μ distribution is an extremely versatile fading model that includes as special cases nearly all linear fading models pertaining to LOS and NLOS scenarios, such as κ-μ ($m \to \infty$), Nakagami-m ($\mu = m$ and $\kappa \to 0$), Rayleigh ($\mu = m = 1$ and $\kappa \to 0$), and Rice ($\mu = 1, \kappa = K$ and $m \to \infty$), to name a few [54, Table I].

As far as the network performance is concerned, we identify two performance regimes in this paper: 1) the noise-limited regime, and 2) the dense interference-limited one. To characterize both, we propose a unified framework analyzing mixed FSO-RF networks over generalized Málaga-$\mathcal{M}$/shadowed κ-μ fading while integrating both user and aperture selections.

A. NETWORK INTERFERENCE MODEL

Emerging technologies advocate statistical interference modeling using spatial point processes to model both the number and the random locations of the interferers. The latters are distributed randomly around each user k at an intensity of λ_k along a PPP Φ_k. The aggregated interference at user k can be expressed as $\mathcal{I}_k = \sum_{j \in \Phi_k} \bar{\gamma}_{j,k} d_{k,j}^{-\nu_j} g_{k,j}$, where $g_{k,j}$ is channel gain between the j-th interferer and the k-th user U_k following shadowed κ-μ distribution with $\mathbb{E}\{g_{k,j}\} = 1$, i.e., $g_{k,j} \sim \mathcal{S}(\kappa_I, m_I, \mu_I, 1/\bar{\gamma}_{\mathcal{I},k})$. By exploiting the statistical independence between small-scale fading and point processes, the aggregated interference has the Laplace transform $\psi_{\mathcal{I}_k}(z) = \mathbb{E}\{e^{-z\mathcal{I}_k}\}$ that is expressed as

$$\psi_{\mathcal{I}_k}(z) = \mathbb{E}\left\{\prod_{j \in \Phi_k} \mathbb{E}\{e^{-z\bar{\gamma}_{j,k} d_{k,j}^{-\nu_j} g_{k,j}}\}\right\}$$
$$= \exp\left[-\lambda_k \left(\bar{\gamma}_{\mathcal{I},k} z\right)^{\frac{2}{\nu}} \Sigma(\nu)\right], \quad \nu > 2 \quad (1)$$

where the path-loss exponent is assumed to be the same for the interfering links (i.e. $v_j = v$). Moreover, using [54] and [55, Eq. (61)] we have

$$\Sigma(v) = \frac{\pi \Gamma\left(1 - \frac{2}{v}\right) \mu^{-\frac{2}{v}} m_I^{m_I} (1 + \kappa_I)^{-\frac{2}{v}}}{\Gamma(m_I)(\mu_I \kappa_I + m_I)^{m_I}}$$

$$\times G_{3,3}^{1,2}\left[\frac{\mu_I \kappa_I}{\mu_I \kappa_I + m_I} \middle| \begin{array}{c} 1 - \mu_I - \frac{2}{v}, 1 - m_I, \frac{1}{2} \\ 0, 1 - \mu_I, \frac{1}{2} \end{array}\right], \quad (2)$$

where $G_{p,q}^{m,n}[\cdot]$ and $\Gamma(\cdot)$ stand for the Meijer-G [56, Eq. (9.301)] and the gamma [56, Eq. (8.310.1)] functions, respectively.

B. USER SELECTION

The pre-user selection SNR following transmit MRT (i.e., the relay uses the optimal transmit weight vector, which is constructed as $w_k = h_k^H / \|h_k\|$, where $h_k = [h_{1,k}, \ldots, h_{M,k}]$ and $(\cdot)^H$ denotes the Hermitian transpose operator) of the link between the relay and the k-th user is obtained as $\sum_{j=1}^{M} h_{j,k} = h_k h_k^H$ that is the sum of i.i.d. shadowed κ-μ rvs with unit mean. When the users are perfectly orthogonal and unaware of the interference, it follows that the post-user selection SIR is given by

$$\gamma_{\mathcal{R}} = \frac{\max_{k=1,\ldots,K}\{\gamma_k\}}{\mathcal{I}_{k*}}, \quad (3)$$

where $\gamma_k = \bar{\gamma}_k \sum_{j=1}^{M} h_{j,k}$ is the combined SNR per user, $\bar{\gamma}_k$ is the average SNR per user, and $\mathcal{I}_{k*} = \mathcal{I}_k$ if the k-th user is selected.[2] On the other hand, when the interference powers at the receiving users are identical, it follows that γ_2 has the same form in (3) but with $\mathcal{I}_{k*} = \mathcal{I}$, for $k = 1, \ldots, K$. In noise-limited scenarios, the post-user selection SNR reduces to $\gamma_2 = \max_{k=1,\ldots,K}\{\gamma_k\}$. From (3) and invoking [54], we can write that $\gamma_k \sim \mathcal{S}(\kappa, m_k = M\tilde{m}_k, \mu_k = M\tilde{\mu}_k, 1/\bar{\gamma}_k)$ with a cumulative distribution function (cdf) given by

$$F_{\gamma_k}(\gamma) = 1 - \sum_{j=0}^{N_k} C_{j,k} e^{-\frac{\gamma}{\Omega_{j,k}}} \sum_{r=0}^{m_{j,k}-1} \frac{1}{r!}\left(\frac{\gamma}{\Omega_{j,k}}\right)^r, \quad (4)$$

where N_k and the set of parameters $\{C_{j,k}, m_{j,k}, \Omega_{j,k}\}$ are expressed in terms of $\bar{\gamma}_k, \kappa_k, \mu_k$, and m_k. If $\mu > m$, then $M = \mu$, $m_j = \mu - m - j + 1$, for $0 \leq j \leq \mu - m$ and $m_j = \mu - j + 1$ for $\mu - m < j \leq \mu$. Otherwise $M = m - \mu$ and $m_j = m - j$. For other coefficients Ω_j and C_j, please refer to [57, Table 1] for more details. Let user b denote the selected

best user such that $\gamma_b = \max\{\gamma_1, \ldots, \gamma_K\}$, then we can show that the complementary cdf (ccdf) of γ_b is given by

$$F_{\gamma_b}^{(c)}(\gamma) = 1 - \prod_{k=1}^{K}\left[1 - \sum_{j=0}^{N_k} C_{j,k} e^{-\frac{\gamma}{\Omega_{j,k}}} \sum_{r=0}^{m_{j,k}-1} \frac{1}{r!}\left(\frac{\gamma}{\Omega_{j,k}}\right)^r\right]$$

$$\overset{(a)}{=} \sum_{\mathcal{S}\setminus\varnothing} \sum_{\mathcal{J}} \sum_{\mathcal{R}} (-1)^{Q-1} C_{\mathcal{S},\mathcal{J},\mathcal{R}} \gamma^{r_{\mathcal{J},\mathcal{R}}} e^{-E_{\mathcal{S},\mathcal{J}}\gamma}, \quad (5)$$

where in (a) $\mathcal{S} = \{s_1, s_2, \ldots, s_Q\}$ is a subset of R, $\sum_{\mathcal{S}}$ is the sum over all possible $\mathcal{S}$, $\sum_{\mathcal{J}} = \sum_{j_{s_1}=1}^{N_{s_1}} \cdots, \sum_{j_{s_Q}=1}^{N_{s_Q}}$, and $\sum_{\mathcal{R}} = \sum_{r_1=1}^{m_{j_{s_1}}-1} \cdots, \sum_{r_Q=1}^{m_{j_{s_Q}}-1}$. Also, we denote $r_{\mathcal{J},\mathcal{R}} = \sum_{p=1}^{Q} r_p$, $E_{\mathcal{S},\mathcal{J}} = \sum_{p=1}^{Q} \Omega_{j_{s_p},s_p}^{-1}$, and $C_{\mathcal{S},\mathcal{J},\mathcal{R}} = \prod_{i=1}^{Q} C_{j_{s_i},s_i} \prod_{p=0}^{Q} \frac{\Omega_{j_{s_p},s_p}^{-r_p}}{r_p!}$. Notice that when $\mathcal{S} = \varnothing$ is an empty set, we have $r_{\mathcal{J},\mathcal{R}} = 0$, $E_{\mathcal{S},\mathcal{J}} = 0$, and $C_{\mathcal{S},\mathcal{J},\mathcal{R}} = 1$. By simply differentiating (3) over γ, the probability density function (pdf) of γ_b can then be written as

$$f_{\gamma_b}(\gamma) = \sum_{\mathcal{S}\setminus\varnothing} \sum_{\mathcal{J}} \sum_{\mathcal{R}} (-1)^Q C_{\mathcal{S}\mathcal{J}\mathcal{R}}(r_{\mathcal{J},\mathcal{R}} - E_{\mathcal{S},\mathcal{J}})$$

$$\times \gamma^{r_{\mathcal{J},\mathcal{R}}-1} e^{-E_{\mathcal{S},\mathcal{J}}\gamma}. \quad (6)$$

C. TRANSMIT APERTURE SELECTION (TAPS)

The selection of the suitable transmit aperture at the serving optical station is implemented to maximize the received signal at the relay. In the case where the transmit apertures are perfectly orthogonal, it follows that the TAPS-based SNR is given by

$$\gamma_{\mathcal{F}} = \mu_r \left(\Xi \max_{l=1,\ldots,L} f_l\right)^r, \quad (7)$$

where f_l is the optical irradiance of the l-th aperture, r is the parameter that describes the detection technique at the relay (i.e. $r = 1$ is associated with heterodyne detection and $r = 2$ is associated with IM/DD), μ_r refers to the electrical SNR of the FSO link and Ξ represents the impairments due to the pointing errors assumed to be equal for all the apertures.

The l-th aperture irradiation f_l follows a Málaga-$\mathcal{M}$ distribution[3] for which the pdf is given by [5, Eq. (24)]

$$f_{I_l}(x) = A \sum_{k=1}^{\beta} a_k x^{\frac{\alpha+k}{2}-1} K_{\alpha-k}\left(2\sqrt{\frac{\alpha\beta x}{g\beta + \phi}}\right), \quad (8)$$

---

[2]The SNR-based user selection is less complex than the SINR-based one since it does not require the knowledge of the interferers' CSI for the identification of the suitable user index. Moreover, both schemes perform the same when the average per-user interference power is the same (i.e., $\mathcal{I}_{k*} = \mathcal{I}$ for $k = 1, \ldots, K$) [53]. The latter is optimal whereas the former is suboptimal.

[3]One of the main motivation to study this turbulence model is its generality i.e. Málaga-$\mathcal{M}$ unifies most of the proposed statistical models characterizing the optical irradiance in homogeneous and isotropic turbulence [5, Table 1], [4]. Hence both $\mathcal{G}$-$\mathcal{G}$ and $\mathcal{K}$ models are special cases of the Málaga-$\mathcal{M}$ distribution, as they mathematically derive from (8) by setting $(g = 0, \phi = 1)$ and $(g \neq 0, \phi = 0$ or $\beta = 1)$, respectively [4].

while the ccdf is obtained in [49, Eq. (11)] as[4]

$$
F_{f_l}^{(c)}(x) = A\sqrt{\pi} \sum_{k=1}^{\beta} \sum_{j=0}^{\alpha-k-\frac{1}{2}} \frac{\psi_{k,j}}{\left(\sqrt{\frac{\alpha\beta}{\mu\beta+\Omega}}\right)^{\alpha+k}}
$$
$$
\times \Gamma\left(\alpha + k - j - \frac{1}{2}, 2\sqrt{\frac{\alpha\beta x}{g\beta + \phi}}\right), \quad (9)
$$

where $A = \alpha^{\frac{\alpha}{2}} (g\beta/(g\beta + \phi))^{\beta+\frac{\alpha}{2}} g^{-1-\frac{\alpha}{2}}$ whereby α, β, g, and ϕ are the fading parameters related to the atmospheric turbulence conditions, $\psi_{k,j} = \frac{a_k(\alpha-k-\frac{1}{2}+j)!2^{\frac{1}{2}-\alpha-k-j}}{(\alpha-k-\frac{1}{2}-j)!j!}$ with $a_k = \binom{\beta-1}{k-1}(g\beta+\phi)^{1-\frac{k}{2}}((g\beta+\phi)/\alpha\beta)^{\frac{\alpha+k}{2}}(\phi/g)^{k-1}(\alpha/\beta)^{\frac{k}{2}}$, and $\Gamma(\cdot,\cdot)$ stands for the upper incomplete Gamma function [56, Eq. (8.350.2)]. Upon substituting the incomplete Gamma function in (9) by its series expansion $\Gamma(n,z) = \Gamma(n)e^{-z}\sum_{j=0}^{n-1}\frac{z^m}{m!}$ [56, Eq. (8.352.2)] and applying the multinomial expansion, the cdf of the first hop SNR $\gamma_{\mathcal{F}}$ can be obtained as

$$
F_{\gamma_{\mathcal{F}}}(\gamma) = \mathbb{E}_{\Xi}\left\{\left[F_{f_l}\left(\frac{1}{\Xi}\left(\frac{\gamma}{\mu_r}\right)^{\frac{1}{r}}\right)\right]^L\right\}
$$
$$
= 1 - \sum_{l=1}^{L}\sum_{\Upsilon}\tau_l \mathbb{E}_{\Xi}\left\{e^{-2l\sqrt{\frac{\alpha\beta\left(\frac{x}{\mu_r}\right)^{\frac{1}{r}}}{\Xi(g\beta+\phi)}}}\left(\frac{\gamma}{\mu_r}\right)^{\frac{\delta_l}{2r}}\left(\frac{1}{\Xi}\right)^{\frac{\delta_l}{2}}\right\},
$$
$$
(10)
$$

where $\sum_{\Upsilon} = \sum_{\Upsilon_{l,\beta}}\sum_{\Upsilon_{lp,\alpha-lp+\frac{1}{2}}}\sum_{\Upsilon_{p_q\alpha+lp-lp_q-\frac{1}{2}}}$, whereby $\Upsilon_{z,l} = \{(z_1,\ldots,z_l): z_i \geqslant 0, \sum_{i=1}^{l}z_i = z\}$; $\delta_l = \sum_{l=0}^{\alpha+lp-lp_q-\frac{3}{2}}lt_{p_{q_{l+1}}}$ and

$$
\tau_t = \prod_{p=1}^{\beta}\prod_{q=1}^{\alpha-t_p+\frac{1}{2}}\prod_{r=1}^{\alpha+t_p-t_{pq}-\frac{1}{2}}\frac{(A\sqrt{\pi})^{t_{pqr}}\binom{L}{t}(-1)^{t+1}t!}{\prod_{k=1}^{\alpha+t_p-t_{pq}-\frac{1}{2}}t_{p_{q_k}}}
$$
$$
\times\left(\psi_{t_p,t_{pqr},t_{pq}}\left(\frac{\alpha\beta}{g\beta+\phi}\right)^{\frac{t_{pqr}-\alpha-t_p-1}{2}}\right)^{t_{pqr}}. \quad (11)
$$

Recalling that $f_\Xi(x) = \frac{\xi^2}{A_0^{\xi^2}}x^{\xi^2-1}$, $0 \leqslant x \leqslant A_0$, where ξ is the ratio between the equivalent beam radius and the pointing error displacement standard deviation (i.e., jitter) at the relay (for negligible pointing errors $\xi \to \infty$), A_0 defines the pointing loss [50]. From (10), the TAPS-based SNR cdf

[4]Note that (8) is valid only for $\alpha = n + \frac{1}{2}$, where n is a positive integer. However, in practice, the obtained results serve as insightful lower and upper bounds for arbitrary values of α. For the other values of α (i.e. $\alpha \neq n + \frac{1}{2}$, $n \in \mathbb{N}$), Hankel's expansion [56] could be considered to accurately approximate the Málaga-$\mathcal{M}$ distribution, yet being beyond the scope of this contribution.

with pointing errors is obtained as

$$
F_{\gamma_{\mathcal{F}}}(\gamma) \stackrel{(a)}{=} 1 - \frac{\xi^2}{A_0^{\xi^2}}\sum_{l=1}^{L}\sum_{\Upsilon}\tau_l\left(\frac{\gamma}{\mu_r}\right)^{\frac{\delta_l}{2r}}\int_0^{A_0}x^{\xi^2-\frac{\delta_l}{2}-1}
$$
$$
\times\mathcal{H}_{0,1}^{1,0}\left[2\,l\sqrt{\frac{\alpha\beta\left(\frac{\gamma}{\mu_r}\right)^{\frac{1}{r}}}{x(g\beta+\phi)}}\,\bigg|\,\begin{matrix}-\\(0,1)\end{matrix}\right]dx, \quad (12)
$$

where (a) follows from substituting the exponential function using $e^{-\sqrt{z}} = \frac{1}{\sqrt{\pi}}\mathcal{H}_{0,2}^{2,0}\left[\frac{z}{4}\,\big|\,\begin{matrix}-\\(0,1),(\frac{1}{2},1)\end{matrix}\right]$, with $\mathcal{H}_{p,q}^{m,n}[\cdot]$ standing for the Fox's H-function [58, Eq. (1.2)]. Applying [58, Eq. (2.53)] to (12) yields

$$
F_{\gamma_{\mathcal{F}}}(\gamma) = 1 - \frac{\xi^2 r}{\sqrt{\pi}}\sum_{l=1}^{L}\sum_{\Upsilon}\tau_l\left(\frac{\gamma}{\widetilde{\mu}_r}\right)^{\frac{\delta_l}{2r}}\mathcal{H}_{1,3}^{3,0}
$$
$$
\times\left[\frac{B^{2r}l^{2r}\gamma}{\widetilde{\mu}_r}\,\bigg|\,\begin{matrix}(\xi^2+1-\frac{\delta_l}{2},r)\\(\xi^2-\frac{\delta_l}{2},r),(0,r),(\frac{1}{2},r)\end{matrix}\right], \quad (13)
$$

where $B = \sqrt{\alpha\beta/g\beta+\phi}$ and $\widetilde{\mu}_r = \mu_r A_0^r$ is the average SNR of the FSO link. Differentiating (13) with respect to γ by applying [58, Eq. (1.69)] yields the pdf of the FSO TAPS SNR as

$$
f_{\gamma_{\mathcal{F}}}(\gamma) = \frac{\xi^2 r}{\sqrt{\pi}}\sum_{l=1}^{L}\sum_{\Upsilon}\frac{\tau_l'}{B^{\delta_l}l^{\delta_l}}\gamma^{-1}\mathcal{H}_{2,4}^{3,1}
$$
$$
\times\left[\frac{B^{2r}l^{2r}\gamma}{\widetilde{\mu}_r}\,\bigg|\,\begin{matrix}(0,1),(\xi^2+1,r)\\(\xi^2,r),(\frac{\delta_l}{2},r),(\frac{1}{2}+\frac{\delta_l}{2},r),(1,1)\end{matrix}\right], \quad (14)
$$

where $\tau_l' = -\tau_l$.

III. ANALYTICAL END-TO-END PERFORMANCE ANALYSIS

Under the assumption of channel-assisted relaying, and following the same procedure as in [59], the end-to-end (e2e) received SNR/SIR γ_{eq} is equivalent to $\gamma_{eq} = \left(\frac{1}{\gamma_{\mathcal{F}}} + \frac{1}{\gamma_{\mathcal{R}}}\right)^{-1}$. In the following, we develop the exact and upper bound expressions for the outage and error rate probabilities of the proposed system model with SNR-based user selection both in noise-limited and interference-limited scenarios. Furthermore, we perform an asymptotic analysis for the outage probability and average error rate at high SNR.

A. OUTAGE PROBABILITY

The outage probability is defined as the probability that the e2e SNR/SIR γ_{eq} falls below a predetermined threshold γ_{th}

$$
P_{\text{out}}(\gamma_{th}) = Pr\left(\gamma_{eq} < \gamma_{th}\right)
$$
$$
= 1 - \gamma_{th}\int_1^\infty Pr\left(\gamma_{\mathcal{R}} > \gamma_{th} + \frac{\gamma_{th}}{u-1}\right)f_{\gamma_{\mathcal{F}}}(u\gamma_{th})\,du, \quad (15)
$$

where $f_{\gamma_{\mathcal{F}}}$ is given in (14), and the term $Pr(\gamma_{\mathcal{R}} > \gamma) = F_{\gamma_{\mathcal{R}}}^{(c)}(\gamma)$ is already obtained in (5) in the noise-limited case.

In the interference-limited case, $Pr(\gamma_R > \gamma) = \mathcal{E}_{\mathcal{I}}\{F_{\gamma_b}^{(c)}(\mathcal{I}\gamma)\}$ will be derived hereafter.

1) NOISE-LIMITED SCENARIO

The outage probability in this case can be expressed as

$$P_{\text{out}}(\gamma_{th})$$

$$= 1 - \frac{\xi^2 r}{\sqrt{\pi}} \sum_{l=1}^{L} \sum_{\Upsilon} \frac{\tau_l'}{B^{\delta_l} l^{\delta_l}} \sum_{\mathcal{S}\backslash\varnothing} \sum_{\mathcal{J}} \sum_{\mathcal{R}} (-1)^{Q-1}$$

$$\times C_{\mathcal{S},\mathcal{J},\mathcal{R}} \sum_{k=0}^{\infty} \frac{(-1)^k}{k!} E_{\mathcal{S},\mathcal{J}}^k \gamma_{th}^{k+r_{\mathcal{J},\mathcal{R}}-1} \mathcal{H}_{0,1:3,1:1,1}^{1,0:2,5:1,2}$$

$$\times \left[\begin{array}{c} \frac{B^{2r}l^{2r}\gamma_{th}}{\widetilde{\mu}_r} \\ -1 \end{array} \middle| \begin{array}{c} (-1:1,1) \\ - \\ (\xi,\Xi);(k+r_{\mathcal{J},\mathcal{R}},1) \\ (\delta,\Delta),(-1,1);(0,1),(k+r_{\mathcal{J},\mathcal{R}}-1,1) \end{array}\right],$$

$$(16)$$

where $\mathcal{H}[\cdot,\cdot]$ denotes the Fox's H-function of two variables [60, Eq. (1.1)], $(\xi,\Xi) = (0,1),(\xi^2+1,r)$ and $(\delta,\Delta) = (\xi^2,r),(\frac{\delta_l}{2},r),(\frac{1}{2}+\frac{\delta_l}{2},r),(1,1)$.

Proof: By plugging (5) and (14) into (15) and relabeling $u = \frac{u-1}{u}$ after using the Taylor series expansion of the exponential function, we obtain

$$P_{\text{out}}(\gamma_{th}) = 1 - \frac{\xi^2 r}{\sqrt{\pi}} \sum_{l=1}^{L} \sum_{\Upsilon} \frac{\tau_l'}{B^{\delta_l} l^{\delta_l}} \sum_{\mathcal{S}\backslash\varnothing} \sum_{\mathcal{J}} \sum_{\mathcal{R}} C_{\mathcal{S}\mathcal{J}\mathcal{R}}$$

$$\times \sum_{k=0}^{\infty} \frac{(-1)^{k+Q}}{k!} E_{\mathcal{S}\mathcal{J}}^k \gamma_{th}^{k+r_{\mathcal{J},\mathcal{R}}-1} \int_0^1 \frac{u^{-k-r_{\mathcal{J},\mathcal{R}}}}{(1-u)^2}$$

$$\times \mathcal{H}_{2,4}^{3,1}\left[\frac{B^{2r}l^{2r}\gamma_{th}}{\widetilde{\mu}_r(1-u)} \middle| \begin{array}{c} (\xi,\Xi) \\ (\delta,\Delta) \end{array}\right] du. \quad (17)$$

Then resorting to [58, Eq. (2.66)] yields (16) after some manipulations.

2) INTERFERENCE-LIMITED SCENARIO

In this case, the term $Pr(\gamma_R > \gamma)$ in (15) is expressed as

$$Pr(\gamma_R > \gamma)$$

$$= \sum_{\mathcal{S}\backslash\varnothing} \sum_{\mathcal{J}} \sum_{\mathcal{R}} (-1)^{Q+r_{\mathcal{J},\mathcal{R}}-1} \frac{C_{\mathcal{S}\mathcal{J}\mathcal{R}}}{(E_{\mathcal{S}\mathcal{J}})^{r_{\mathcal{J},\mathcal{R}}}}$$

$$\times \mathcal{H}_{1,2}^{2,0}\left[A_{\mathcal{I}}(E_{\mathcal{S}\mathcal{J}}\gamma)^{\frac{2}{\nu}} \middle| \begin{array}{c} (0,\frac{2}{\nu}) \\ (r_{\mathcal{J},\mathcal{R}},\frac{2}{\nu}),(0,1) \end{array}\right], \quad (18)$$

where $A_{\mathcal{I}} = \lambda(\bar{\gamma}_{\mathcal{I}})^{\frac{2}{\nu}}\Sigma(\nu)$, or alternatively as

$$Pr(\gamma_R > \gamma)$$

$$= \sum_{\mathcal{S}\backslash\varnothing} \sum_{\mathcal{J}} \sum_{\mathcal{R}} (-1)^{Q+r_{\mathcal{J},\mathcal{R}}-1} \frac{C_{\mathcal{S}\mathcal{J}\mathcal{R}}}{(E_{\mathcal{S}\mathcal{J}})^{r_{\mathcal{J},\mathcal{R}}}}$$

$$\times \sum_{j=0}^{\infty} \sum_{k=0}^{r_{\mathcal{J},\mathcal{R}}} \frac{(-1)^{k+j}\Phi_k}{j!} A_{\mathcal{I}}^{k+j}(E_{\mathcal{S}\mathcal{J}}\gamma)^{\frac{2}{\nu}(k+j)}. \quad (19)$$

Proof: See Appendix A.

Substituting the resulting expression of $Pr(\gamma_R > \gamma)$ for $\gamma = \gamma_{th} + \frac{\gamma_{th}}{u-1}$ into (15) and making a Taylor expansion of the power term, we infer that

$$P_{\text{out}}(\gamma_{th})$$

$$= 1 - \frac{\xi^2 r}{\sqrt{\pi}} \sum_{l=1}^{L} \sum_{\Upsilon} \frac{\tau_l}{\widetilde{\mu}_r^{\frac{\delta_l}{2r}}} \sum_{\mathcal{S}\backslash\varnothing} \sum_{\mathcal{J}} \sum_{\mathcal{R}} \Pi_{\mathcal{S}\mathcal{J}\mathcal{R}}$$

$$\times \sum_{k=0}^{r_{\mathcal{J},\mathcal{R}}} \sum_{j=0}^{\infty} \frac{(-1)^{k+j}\Phi_k}{j!} A_{\mathcal{I}}^{k+j} E_{\mathcal{S},\mathcal{J}}^{\frac{2}{\nu}(k+j)} \gamma_{th}^{\frac{2}{\nu}(k+j)+\frac{\delta_l}{2r}} \mathcal{T}_{k,j},$$

$$(20)$$

where $\Pi_{\mathcal{S}\mathcal{J}\mathcal{R}} = (-1)^{Q+r_{\mathcal{J},\mathcal{R}}-1} \frac{C_{\mathcal{S}\mathcal{J}\mathcal{R}}}{E_{\mathcal{S}\mathcal{J}}^{r_{\mathcal{J},\mathcal{R}}}}$, and $\mathcal{T}_{k,j}$ is given by

$$\mathcal{T}_{k,j} = \left(\frac{B^{2r}l^{2r}\gamma_{th}}{\widetilde{\mu}_r}\right)^{-\frac{\delta_l}{2r}} \int_1^{\infty} \frac{u^{\frac{2}{\nu}(k+j)-1}}{(u-1)^{\frac{2}{\nu}(k+j)}}$$

$$\times \mathcal{H}_{2,4}^{3,1}\left[\frac{B^{2r}l^{2r}u\gamma_{th}}{\widetilde{\mu}_r} \middle| \begin{array}{c} (\xi,\Xi) \\ (\delta,\Delta) \end{array}\right] du. \quad (21)$$

Finally, applying [58, Eq. (2.54)] yields the desired result for the outage probability as

$$P_{\text{out}}(\gamma_{th})$$

$$= 1 - \frac{\xi^2 r}{\sqrt{\pi}} \sum_{l=1}^{L} \sum_{\Upsilon} \frac{\tau_l}{B^{\delta_l} l^{\delta_l}} \sum_{\mathcal{S}\backslash\varnothing} \sum_{\mathcal{J}} \sum_{\mathcal{R}} \Pi_{\mathcal{S}\mathcal{J}\mathcal{R}}$$

$$\times \sum_{k=0}^{r_{\mathcal{J},\mathcal{R}}} \sum_{j=0}^{\infty} \frac{(-1)^{k+j}\Gamma\left(1-\frac{2}{\nu}(k+j)\right)}{j!} \Phi_k A_{\mathcal{I}}^{k+j} E_{\mathcal{S}\mathcal{J}}^{\frac{2}{\nu}(k+j)}$$

$$\times \gamma_{th}^{\frac{2}{\nu}(k+j)} \mathcal{H}_{3,5}^{4,1}\left[\frac{B^{2r}l^{2r}\gamma_{th}}{\widetilde{\mu}_r} \middle| \begin{array}{c} (\xi,\Xi),(1-\frac{2}{\nu}(k+j),1) \\ (\delta,\Delta) \end{array}\right].$$

$$(22)$$

It should be noted γ_{eq} can be upper bounded as

$$\gamma_{eq} \leq \gamma_{ub} = \min\{\gamma_{\mathcal{F}}, \gamma_{\mathcal{R}}\}. \quad (23)$$

For the considered TAPS/user selection relay system, the use of the upper bound γ_{ub} leads to lower bounds for the outage probability at the selected user. Note that (23) corresponds to a mixed FSO-RF AF relaying system with cochannel interference when using (18). Consequently, the outage probability of the considered system can be lower bounded based on

$$P_{\text{out}}^{lb}(\gamma_{th}) = Pr[\gamma_{ub} < \gamma_{th}] = F_{\gamma_{ub}}(\gamma_{th})$$

$$= 1 - \prod_{X\in\{\mathcal{F},\mathcal{R}\}} F_{\gamma_X}^{(c)}(\gamma_{th}), \quad (24)$$

where $F_{\gamma_X}^{(c)}(\gamma_{th})$, $X \in \{\mathcal{F},\mathcal{R}\}$ are already derived in (13), (5), and (18) under both noise-limited and interference-limited scenarios.

`Special Cases`: Without interference, it can be shown for $L = K = 1$ (i.e., Málaga-$\mathcal{M}$/shadowed κ-μ fading) that (16) simplifies to [18, Eq. (19)]. For $L = 1$, $m_k = \mu_k$, $\mu_k = 2\mu$, $\kappa_k = (1-\eta_k)/2\eta_k$, and $k = 1,\ldots,K$, (i.e., Málaga-$\mathcal{M}$/ multiuser η-μ fading), the CDF in (16) simplifies to [50, Eq. (22)] and to [45, Eq. (21)] when $g = 0$, $\phi = 1$,

and $\kappa_k \rightarrow \infty$ (i.e., Gamma-Gamma/multiuser Nakagami-m fading). With PPP interference, the CDF in (22) extends existing performance analysis framework (cf. [53] and references therein) to encompass FSO-based backhauling through the implementation of aperture selection over generalized Málaga-$\mathcal{M}$ atmospheric turbulence fading.

B. EXACT AVERAGE SYMBOL ERROR PROBABILITY

The average SEP performance at the best user is

$$\mathcal{B} = a \int_0^\infty \sqrt{\frac{b}{t}} \, \mathcal{J}_{-1}\left(2\sqrt{bt}\right) \mathcal{M}_{\gamma_{\mathcal{R}}^{-1}}(t) \, \mathcal{M}_{\gamma_{\mathcal{F}}^{-1}}(t) \, dt, \quad (25)$$

where $\mathcal{M}_{1/\gamma_X}(s)$, $X \in \{\mathcal{F}, \mathcal{R}\}$ is the MGF of the inverse SNR/SIR of the first and second hops, respectively. Moreover, a and b are parameters for different M-ary modulations, and $\mathcal{J}_{-1}$ is the Bessel function of the first kind [56]. In what follows, $\mathcal{M}_{1/\gamma_X}(s)$ are obtained directly from the ccdfs as $\mathcal{M}_{1/\gamma_X}(s) = s \int_0^\infty t^{-2} e^{-s/t} F_X^{(c)}(t) dt$, where $F_X^{(c)}(t)$, $X \in \{\mathcal{R}, \mathcal{F}\}$. In the FSO link, exploiting (13) and recognizing that $\exp(-x) = H_{0,1}^{1,0}\left[x \Big|_{(0,1)}^{-}\right]$ [58, Eq. (1.125)], $\mathcal{M}_{1/\gamma_{\mathcal{F}}}(s)$ is expressed using the Fox's H-function properties [58, Eq. (1.58)] and applying [58, Eq. (2.3)], thereby yielding

$$M_{\gamma_{\mathcal{F}}^{-1}}(s) = \frac{\xi^2 r}{s\sqrt{\pi}} \sum_{l=1}^{L} \sum_{\Upsilon} \frac{\tau_l'}{B^{\frac{\delta_l}{2}} l^{\delta_l}}$$
$$\times \mathcal{H}_{1,4}^{4,0}\left[\frac{B^r l^{2r} s}{\widetilde{\mu}_r} \Big|_{(\delta, \Delta)}^{(\xi^2 + 1 - \frac{\delta_l}{2}, r)}\right]. \quad (26)$$

1) NOISE-LIMITED SCENARIO
In this case the expression of $M_{1/\gamma_{\mathcal{R}}}(s)$ is obtained from (5) by relying on the very same approach adopted in (26) and applying [58, Eq. (2.3)] as

$$M_{\gamma_{\mathcal{R}}^{-1}}(s) = \sum_{\mathcal{S}\backslash\varnothing} \sum_{\mathcal{J}} \sum_{\mathcal{R}} (-1)^{Q-1} \frac{s \, C_{\mathcal{S}\mathcal{J}\mathcal{R}}}{E_{\mathcal{S}\mathcal{J}}^{r_{\mathcal{J},\mathcal{R}}-1}}$$
$$\times \mathcal{H}_{0,2}^{2,0}\left[E_{\mathcal{S}\mathcal{J}} s \Big|_{(r_{\mathcal{J},\mathcal{R}}-1,1),(0,1)}^{-}\right]. \quad (27)$$

Substituting the last expression with (26) into (25) and applying [60, Eq. (2.1)] with $J_{-1}(z) = H_{0,2}^{1,0}\left[\frac{z^2}{4}\Big|_{(-\frac{1}{2},1),(\frac{1}{2},1)}^{-}\right]$ [58, Eq. (1.127)], yield the exact error probability expression is given in (28), as shown at the bottom of this page.

2) INTERFERENCE-LIMITED SCENARIO
In this case the expression of $M_{1/\gamma_{\mathcal{R}}}(s)$ is obtained from (18) after applying [58, Eq. (2.3)] as

$$M_{\gamma_{\mathcal{R}}^{-1}}(s) = \sum_{\mathcal{S}\backslash\varnothing} \sum_{\mathcal{J}} \sum_{\mathcal{R}} (-1)^{Q+r_{\mathcal{J},\mathcal{R}}-1} \frac{C_{\mathcal{S}\mathcal{J}\mathcal{R}}}{(E_{\mathcal{S}\mathcal{J}})^{r_{\mathcal{J},\mathcal{R}}}} \mathcal{H}_{1,3}^{3,0}$$
$$\times \left[A_{\mathcal{I}}\left(E_{\mathcal{S}\mathcal{J}} s\right)^{\frac{2}{v}} \Big|_{(r_{\mathcal{J},\mathcal{R}}, \frac{2}{v}), (0,1), (1, \frac{2}{v})}^{(0, \frac{2}{v})}\right]. \quad (29)$$

Substituting the last expression with (26) into (25) and following the same steps as in (28) yield the error rate performance in interference-limited scenario is given in (30), as shown at the bottom of this page.

The e2e upper bound of the error rate probability for bi-dimensional modulation type can be obtained using the MGF-based technique as [61, Eq. (5)]

$$\mathcal{B}_{\mathrm{u}p} = \frac{\beta_M}{\pi} \sum_{p=1}^{\tau_M} \int_0^{\pi/2} M_{\gamma_{ub}}\left(\frac{a_p^2}{2\sin^2(\theta)}\right) d\theta, \quad (31)$$

where β_M, a_p, and τ_M are modulation-dependent parameters. Using the expression for $\mathcal{M}_{\gamma_{ub}}(s) = s \int_0^\infty e^{-st} F_{\gamma_{ub}}(t) dt$, where $F_{\gamma_{ub}}(\cdot)$ is given in (24) using the alternative expression of $Pr(\gamma_{\mathcal{R}} > \gamma)$ shown in (19), the obtained expression for $\mathcal{M}_{\gamma_{ub}}$ follows from invoking the Laplace transform of the Fox's $\mathcal{H}$-function [58, Eq. (2.19)]. Inserting the obtained expression into (31) gives the expression for $\mathcal{B}_{\mathrm{u}p}$ in

$$\mathcal{B} = \frac{\xi^2 ar}{\sqrt{\pi}} \sum_{l=1}^{L} \sum_{\Upsilon} \frac{\tau_l'}{B^{\frac{\delta_l}{2}} l^{\delta_l}} \sum_{\mathcal{S}\backslash\varnothing} \sum_{\mathcal{J}} \sum_{\mathcal{R}} (-1)^{Q-1} \frac{C_{\mathcal{S},\mathcal{J},\mathcal{R}}}{E_{\mathcal{S},\mathcal{J}}^{r_{\mathcal{J},\mathcal{R}}-1}} \times \mathcal{H}_{2,[0:1],0,[2:4]}^{1,0,0,2,4}\left[\begin{array}{c}\frac{E_{\mathcal{S},\mathcal{J}}}{b} \\ \frac{B^r l^{2r} \gamma}{\widetilde{\mu}_r b}\end{array}\Bigg|\begin{array}{c}(0,1),(1,1) \\ -, (\xi^2 + 1 - \frac{\delta_l}{2}, r) \\ \\ - \\ (r_{\mathcal{J},\mathcal{R}}-1,1),(0,1),(\delta,\Delta)\end{array}\right] \quad (28)$$

$$\mathcal{B} = \frac{\xi^2 avr}{2\sqrt{\pi}} \sum_{l=1}^{L} \sum_{\Upsilon} \frac{\tau_l}{(b\mu_r)^{\delta_l/2r}} \sum_{\mathcal{S}\backslash\varnothing} \sum_{\mathcal{J}} \sum_{\mathcal{R}} \Pi_{\mathcal{S},\mathcal{J},\mathcal{R}}$$
$$\times \mathcal{H}_{0,[1:1],0,[4:3]}^{2,0,0,4,3}\left[\begin{array}{c}\frac{B^r l^{2r}\gamma}{\widetilde{\mu}_r b} \\ A_{\mathcal{I}}^{v/2}\frac{E_{\mathcal{S}\mathcal{J}}}{b}\end{array}\Bigg|\begin{array}{c}(\frac{\delta_l}{2r}, 1), (\frac{1-\delta_l}{2r}, 1) \\ (\xi^2 + 1 - \frac{\delta_l}{2}, r), (0, \frac{2}{v}) \\ \\ - \\ (\xi^2 - \frac{\delta_l}{2}, r), (0,r), (\frac{1}{2}, r), (1 - \frac{\delta_l}{2}, 1), (r_{\mathcal{J},\mathcal{R}}, \frac{2}{v}), (0,1), (1, \frac{2}{v})\end{array}\right] \quad (30)$$

interference-limited regime after relabeling $t = \sin^2(\theta)$ as

$$
\begin{aligned}
&\mathcal{B}_{\mathrm{u}p} \\
&= \frac{\beta_M \xi^2 r}{2\sqrt{\pi}\pi} \sum_{p=1}^{\tau_M}\sum_{l=1}^{L}\sum_{\Upsilon} \tau_l \left(\frac{a_p^2}{2\widetilde{\mu}_r}\right)^{\frac{\delta_l}{2r}} \sum_{\mathcal{S}\backslash\varnothing}\sum_{\mathcal{J}}\sum_{\mathcal{R}} \Pi_{\mathcal{S},\mathcal{J},\mathcal{R}} \\
&\times \sum_{k=0}^{r_{\mathcal{J},\mathcal{R}}}\sum_{j=0}^{\infty} \frac{(-1)^{k+j}\Phi_k A_{\mathcal{I}}^{k+j}}{j!\left(\frac{a_p^2}{2}E_{\mathcal{S},\mathcal{J}}\right)^{-\frac{2}{\nu}(k+j)}} \int_0^1 \frac{t^{\frac{2}{\nu}(k+j)+\frac{\delta_l}{2r}-\frac{1}{2}}}{\sqrt{1-t}} \\
&\times \mathcal{H}_{2,3}^{3,1}\left[\frac{a_p^2 B^{2r} l^{2r} t}{2\widetilde{\mu}_r}\middle|\begin{array}{l}(-\frac{2}{\nu}(k+j)-\frac{\delta_l}{2r},1),(\xi^2+1-\frac{\delta_l}{2},r)\\(\xi^2-\frac{\delta_l}{2},r),(0,r),(\frac{1}{2},r)\end{array}\right] dt.
\end{aligned}
$$
(32)

Finally, resorting to [58, Eq. (2.53)] we obtain a closed-form expression for $\mathcal{B}_{\mathrm{u}p}$ in (33), as shown at the bottom of this page.

`Special Cases:` As a special case, it can be shown in noise-limited scenarios that (28) provides an exact alternative expression to the approximate one for the SEP obtained in [50, Eq. (22)] if we set $L = 1$, $m_k = \mu_k$, $\mu_k = 2\mu$, $\kappa_k = (1-\eta_k)/2\eta_k$, and $k = 1, \ldots, K$, (i.e., Málaga-$\mathcal{M}$/multiuser η-μ fading). For $K = 1$, $m = \mu = 1$, the SEP in (28) simplifies to [22, Eq. (32)] obtained at high SNR for multi-aperture Málaga-$\mathcal{M}$/Rayleigh fading channels. For $L = K = 1$, $g = 0$, $\phi = 1$, and $m = \mu$ (i.e., Gamma-Gamma/Nakagami-m fading), the SEP in (28) simplifies to [7, Eq. (39)]. In interference-limited scenarios, the SEP in (30), to the best to our knowledge, provides a novel performance framework for dense small-cell deployments, in which BSs are connected to the core network through an FSO-based backhaul. To this end, we adopt the generic Málaga-$\mathcal{M}$/shadowed κ-μ fading to encompass the full range of turbulence conditions/shadowed LOS and NLOS cases that cover most notably, as will be shown in section VI, the compelling case of mixed FSO/mmWave.

`Remark:` The derived analytical expressions for the outage probability and SEP in (16), (22), (28), and (30) are highly generic and novel and can be easily mapped into most existing irradiance and fading models. Notably, the end-to-end average SEP expressions in (28) and (30) are obtained via finite sums of bivariate Fox's H-functions, for which efficient implementation codes exists in most popular mathematical software packages. Hence, such expressions can be very rapidly and efficiently computed. Yet, although the derived outage expressions in (16) and (22) consist of infinite series, they converge within a finite number of about a dozen summations, regardless of the average SNRs/SIRs and

turbulence/fading setting. These expressions offer highly efficient analytical tools and stand out as much reliable and faster alternatives to time-consuming Monte-Carlo simulations.

IV. ASYMPTOTIC ANALYSIS

In an effort to understand the impact of some key system parameters on the outage and error rate probabilities, we analyze the asymptotic regime at the high optical SNR $\widetilde{\mu}_r$ and RF SNR $\bar{\gamma} \to \infty$, from which we derive the diversity and coding gains. The following subsections address the asymptotic behaviour both of the outage and error rate probabilities and characterize the performance both of the noise-limited and interference-limited regimes and analyze in detail the factors that affect the performance trend.

A. OUTAGE PROBABILITY
Using the lower bound in (23), P_{out} can be approximated at high SNR/SIR as

$$P_{\mathrm{out}}^{\infty} \approx F_{\gamma_{\mathcal{F}}}^{\infty}(\gamma_{th}) + F_{\gamma_{\mathcal{R}}}^{\infty}(\gamma_{th}).\tag{34}$$

1) NOISE-LIMITED SCENARIO
The asymptotic outage probability with the use of opportunistic user scheduling at the RF link and TAPS at the FSO link is derived as

$$
\begin{aligned}
P_{\mathrm{out}}^{\infty} &\approx (\mathcal{G}_c \bar{\gamma})^{-\mathcal{G}_d} \tag{35}\\
&\approx \frac{(\mu(1+\kappa))^{K\mu}}{\left(\frac{\mu\kappa+m}{m}\right)^{Km}(\mu-1)!^K}\left(\frac{\gamma_{th}}{\bar{\gamma}}\right)^{K\mu}\\
&\quad + \Lambda\left(\frac{\gamma_{th}}{\widetilde{\mu}_r}\right)^{\min\left(\frac{\xi^2}{r},\frac{L\beta}{r},\frac{L\alpha}{r}\right)},
\end{aligned}\tag{36}
$$

where

$$
\frac{\Lambda}{\xi^2} = \begin{cases} 2\sum_{p=1}^{L}\binom{L}{p}\frac{(-A\sqrt{\pi})^p}{(2Bp)^{-2\xi^2}}\widetilde{\sum}_k\widetilde{\sum}_i\widetilde{\sum}_j\Xi_1, & \delta = \frac{\xi^2}{r}; \\ \left(\frac{A\sqrt{\pi}2^{2\beta-1}\psi_{\beta,\alpha-\beta-\frac{1}{2}}}{B^{\alpha-\beta}(\xi^2-\beta)}\right)^L, & \delta = \frac{L\beta}{r}; \\ \left(\frac{A\sqrt{\pi}2^{2\alpha-1}\psi_{\beta,\beta-\alpha-\frac{1}{2}}}{B^{\alpha-\beta}(\xi^2-\alpha)}\right)^L, & \delta = \frac{L\alpha}{r}, \end{cases}\tag{37}
$$

where $\Xi_1 = \prod_{t=1}^{p}\frac{\Psi_{k_t,i_t}\Gamma(\alpha+k_t-i_t-\frac{1}{2})}{B^{\alpha+k_t}p^{i_t}j_t!}\Gamma\left(\sum_{t=1}^{p}j_t-2\xi^2\right)$ and $\delta = \min\left(\frac{\xi^2}{r},\frac{L\beta}{r},\frac{L\alpha}{r}\right)$.

Proof: See Appendix B.

$$
\begin{aligned}
\mathcal{B}_{\mathrm{u}p} &= \frac{\beta_M \xi^2 r}{2\pi} \sum_{p=1}^{\tau_M}\sum_{l=1}^{L}\sum_{\Upsilon} \tau_l \left(\frac{a_p^2}{2\widetilde{\mu}_r}\right)^{\frac{\delta_l}{2r}} \sum_{\mathcal{S}\backslash\varnothing}\sum_{\mathcal{J}}\sum_{\mathcal{R}} \Pi_{\mathcal{S},\mathcal{J},\mathcal{R}} \sum_{k=0}^{r_{\mathcal{J},\mathcal{R}}}\sum_{j=0}^{\infty} \frac{(-1)^{k+j}}{j!}\Phi_k A_{\mathcal{I}}^{k+j}\left(\frac{a_p^2}{2}E_{\mathcal{S}\mathcal{J}}\right)^{\frac{2}{\nu}(k+j)}\\
&\times \mathcal{H}_{3,4}^{3,2}\left[\frac{a_p^2 B^r l^{2r}}{2\widetilde{\mu}_r}\middle|\begin{array}{l}(\frac{1}{2}-\frac{2}{\nu}(k+j)-\frac{\delta_l}{2r},1),(-\frac{2}{\nu}(k+j)-\frac{\delta_l}{2r},1),(\xi^2+1-\frac{\delta_l}{2},r)\\(\xi^2-\frac{\delta_l}{2},r),(0,r),(\frac{1}{2},r),(-\frac{2}{\nu}(k+j)-\frac{\delta_l}{2r},1)\end{array}\right]
\end{aligned}\tag{33}
$$

Notice in (36) that $\mathcal{G}_d$ stands for the diversity gain and is defined as the slope of the asymptotic curve, and $\mathcal{G}_c$ is the coding gain representing the SNR advantage of the asymptotic curve relative to $\bar{\gamma}^{-\mathcal{G}_d}$ reference. Comparing (35) with (36), the achievable diversity gain is expressed as $\mathcal{G}_d = \min\{\frac{\xi^2}{r}, \frac{L\beta}{r}, \frac{L\alpha}{r}, K\mu\}$. This result shows that the diversity order is dependent of the worst channel link between the RF and FSO links [18]. For large values of the RF link parameters (i.e., μ and K), and under strong turbulence conditions, pointing errors and a small number of apertures L, the first-hop channel will be dominating the system performance, and hence, the effect the second-hop fading parameters and number of users on the system performance will be extremely minor. In the special case where $m = \mu$, the first term in the RHS of (36) reduces to the asymptotic cdf of the post-user selection SNR in Nakagami-m fading given by $\frac{m^{Km}}{\Gamma(m)^K}\left(\frac{\gamma_{th}}{\bar{\gamma}}\right)^{Km}$, and $\mathcal{G}_d$ coincides with a previously obtained result in [48] when $L = 1$. It is worthwhile to mention here that the MRT scheme employed at the M-antenna relay improves the diversity gain which is in fact given by $KM\tilde{\mu}$ with $\tilde{\mu}$ being the effective fading parameter between the M-antennas relay and the selected user as defined after (3).

2) INTERFERENCE-LIMITED SCENARIO
In this case the asymptotic outage probability is obtained as

$$P_{\text{out}}^{\infty} \approx \frac{A_{\mathcal{I}} \left(\frac{\mu\kappa+m}{m\mu(1+\kappa)}\right)^{-\frac{2}{\nu}}}{\Gamma\left(-\frac{2}{\nu}\right)} \Upsilon \left(\frac{\gamma_{th}}{\bar{\gamma}}\right)^{\frac{2}{\nu}}$$
$$+ \Lambda \left(\frac{\gamma_{th}}{\tilde{\mu}_r}\right)^{\min\left(\frac{\xi^2}{r}, \frac{L\beta}{r}, \frac{L\alpha}{r}\right)}, \quad (38)$$

where $\Upsilon = \sum_{p=1}^{K}\binom{K}{p}p^{\frac{2}{\nu}}(-1)^{p+1}\sum_{j_1=0}^{m-\mu}\cdots\sum_{j_p=0}^{m-\mu}\prod_{n=1}^{p}C_{j_n}$ $\sum_{r_1=0}^{m_{j_1}}\cdots\sum_{r_p=0}^{m_{j_p}}\prod_{n=1}^{p}\left(\frac{p^{-r_n}}{r_n!}\right)\Gamma\left(\sum_{n=1}^{p}r_n-\frac{2}{\nu}\right)$.
   Proof: See Appendix B.

From the above expression, the diversity gain for the outage probability is given by $\mathcal{G}_d = \min\{\frac{\xi^2}{r}, \frac{L\alpha}{r}, \frac{L\beta}{r}, \frac{2}{\nu}\}$. It can be observed that, since $2 \le \nu \le 5$, $\frac{2}{\nu}$ varies from 1 to 2/5; therefore, the condition $\min\{\frac{\xi^2}{r}, \frac{L\alpha}{r}, \frac{L\beta}{r}\} < \frac{2}{\nu}$ implies that the first hop FSO signal is subject to severe pointing conditions $\frac{\xi^2}{r} \le 1$ (i.e., $\xi < 1$ for heterodyne detection with $r = 1$ and $\xi < \sqrt{2}$ for IMDD detection with $r = 2$). Consequently, only in this case the diversity order is determined by $\frac{\xi^2}{r}$; otherwise, the diversity order is determined by $\frac{2}{\nu}$ and decreases as ν increases implying that the outage probability performance is dominated by the effect of the path-loss of the interference sources. In the special case where $m = \mu$ and $K = 1$, we have $\Upsilon = -\frac{\Gamma\left(m-\frac{2}{\nu}\right)}{\Gamma(m)}$ and the first term in the RHS of (38) boils down to the asymptotic cdf of the SIR in PPP interference-limited Nakagami-m fading given by $\frac{A_{\mathcal{I}}\Gamma(m-\frac{2}{\nu})}{\Gamma(m)\Gamma\left(1-\frac{2}{\nu}\right)}\left(\frac{m\gamma_{th}}{\bar{\gamma}}\right)^{\frac{2}{\nu}}$, which is in agreement with previously obtained results in [62, Eq. (56)] and [53].

Another insightful asymptotic performance stems from fixing the average SNR in either RF or FSO link while varying the other SNR. Here, we assume that the average electrical SNR of the FSO link ($\tilde{\mu}_r$) goes to infinity for a fixed and finite valued average SNR/SIR per user in the RF link. Then applying [66, Eq. (1.8.4)] to (24) yields the outage probability of the end-to-end SNR/SINR in the asymptotic regime as

$P_{\text{out}}(\gamma_{th})$

$$\underset{\tilde{\mu}\gg 1}{\approx} 1 - F_{\gamma_{\mathcal{R}}}^{(c)}(\gamma_{th}) \Bigg[\frac{\xi^2 r}{\sqrt{\pi}} \sum_{l=1}^{L}\sum_{\Upsilon} \frac{\tau_l}{B^{\delta_l}l^{\delta_l}}$$
$$\times \sum_{j=1}^{3} \frac{\prod_{i=1,i\neq j}^{3}\Gamma\left(\delta_i-\delta_j\frac{\Delta_i}{\Delta_j}\right)}{\Gamma\left(\xi^2+1-\delta_j\frac{r}{\Delta_j}\right)} \left(\frac{B^{2r}l^{2r}\gamma_{th}}{\tilde{\mu}_r}\right)^{\frac{\delta_j}{\Delta_j}} \Bigg], \quad (39)$$

where $F_{\gamma_{\mathcal{R}}}^{(c)}(\gamma)$ is given in (5) and (18) under noise-limited and interference-limited scenarios. Note that, in comparison to (16) and (22), (39) alleviate the need for infinite series of Fox's H-functions, thereby providing highly efficient analytical tools. It should be noted that the asymptotic expression for the outage probability in (39) is dominated by the effects of the RF link at high FSO SNRs. Moreover, it can be shown using (39) that the diversity order is equal to $\mathcal{G}_d = 0$ meaning that the outage probability curves will saturate at high SNRs and increasing the SNR does not improve the system performance.

B. ASYMPTOTIC AVERAGE SEP
The asymptotic error probability is obtained using the MGF approach for the asymptotic $F_{\gamma_{ub}}(\gamma_{th})$ obtained in (36) that gives the asymptotic MGF in the noise-limited scenario as

$$M_{\gamma_{ub}}^{\infty}(s) \approx \Lambda_1 \frac{\Gamma\left(1+\min\{K\mu, \delta\}\right)}{s^{\min\{K\mu, \delta\}}}\left(\frac{1}{\bar{\gamma}}\right)^{\min\{K\mu, \delta\}}. \quad (40)$$

While in the interference-limited scenario it becomes

$$M_{\gamma_{ub}}^{\infty}(s) \approx \Lambda_2 \frac{\Gamma\left(1+\min\left\{\frac{2}{\nu}, \delta\right\}\right)}{s^{\min\left\{\frac{2}{\nu}, \delta\right\}}}\left(\frac{1}{\bar{\gamma}}\right)^{\min\left\{\frac{2}{\nu}, \delta\right\}}, \quad (41)$$

where Λ_1 and Λ_2 are constants obtained by matching $\mathcal{M}_{\gamma_{ub}}(s) = 1 - s\int_0^{\infty}e^{-st}(1-P_{\text{out}}^{\infty}(t))dt$ with (40) and (41) when $\bar{\gamma} = \tilde{\mu}_r$. Inserting the obtained asymptotic MGF into (31), the asymptotic error probability is expressed as

$$\mathcal{B}^{\infty} = \frac{\beta_M \Psi}{\pi}\sum_{p=1}^{\tau_M} \begin{cases} \dfrac{\Lambda_1\Gamma\left(1+\min\{K\mu, \delta\}\right)}{\left(\frac{1}{a_p^2\bar{\gamma}}\right)^{-\min\{K\mu, \delta\}}}, & \mathcal{I}=0; \\[4mm] \dfrac{\Lambda_2\Gamma\left(1+\min\left\{\frac{2}{\nu}, \delta\right\}\right)}{\left(\frac{1}{a_p^2\bar{\gamma}}\right)^{-\min\left\{\frac{2}{\nu}, \delta\right\}}}, & \mathcal{I}\neq 0 \end{cases} ; \quad (42)$$

where $\Psi = \int_0^{\pi/2} \sin^2(\theta)^{\mathcal{G}_d} d\theta = \frac{\sqrt{\pi}\Gamma(\mathcal{G}_d + \frac{1}{2})}{2\Gamma(\mathcal{G}_d+1)}$. As can be observed from (42), the considered system under noise-limited and interference-limited scenarios has the same diversity gain only when $\nu = 2$, $K = 1$, and $\mu = 1$ (Rayleigh or Rice fading), with an SINR gap between the two scenarios that depends on the coding gain given by $10 \log_{10}(\Lambda_1/\Lambda_2)$ dB.

Exploiting the SEP upper bound in (33) while resorting to the asymptotic expansion of the Fox's H-function [58, Eq. (1.8.1)] $\mathcal{H}_{p,q}^{m,n}(x) \underset{x\to 0}{\approx} x^c$, where $c = \min\limits_{j=1,\dots,m}\left[\frac{\mathfrak{R}(b_j)}{B_j}\right]$, yields

$$\mathcal{B}^\infty = \frac{\beta_M \xi^2 r A_{\mathcal{I}}}{2\pi} \sum_{p=1}^{\tau_M}\sum_{l=1}^{L}\sum_{\Upsilon} \tau_l \sum_{\mathcal{S}\setminus\varnothing}\sum_{\mathcal{J}} \Pi_{\mathcal{S}\mathcal{J}\mathcal{R}} \frac{E_{\mathcal{S}\mathcal{J}}^{\min\left\{\frac{2}{\nu}, r_{\mathcal{J},\mathcal{R}}\right\}}}{\tilde{\mu}_r^{\min\left\{\frac{\xi^2}{r}, \frac{\delta_l}{2r}\right\}}}$$

$$\times \left(\frac{2}{a_p^2}\right)^{\min\left\{\frac{2}{\nu}, r_{\mathcal{J},\mathcal{R}}, \frac{\xi^2}{r}, \frac{\delta_l}{2r}\right\}}$$

$$\times \Gamma\left(1 + \min\left\{\frac{2}{\nu}, r_{\mathcal{J},\mathcal{R}}, \frac{\xi^2}{r}, \frac{\delta_l}{2r}\right\}\right), \qquad (43)$$

thereby corroborating (42).

V. RELAY ASSISTED TAPS/USER SELECTION OPTIMUM DESIGN

This section addresses the optimum resource allocation strategies including power and position allocation. We denote the distance between the K users and the relay by $d_{\mathcal{R}}$, while the distance between the relay and the optical source by $d_{\mathcal{F}}$. Under the scenario where the RF received power decays with the distance, the average value of the per user average SNR is expressed as $\bar{\gamma} = P_{\mathcal{R}} d_{\mathcal{R}}^{-\theta}$, where $P_{\mathcal{R}}$ is the power of the signal per user and θ is the path loss exponent on the RF link. According to Beer-Lambert law [63], the optical beam power has an exponential decay with propagation distance with $\tilde{\mu}_r = P_{\mathcal{F}}e^{-\sigma d_{\mathcal{F}}}$, where δ is the overall attenuation coefficient. To proceed with the analysis, two constraints are assumed including the total signal power of the two hops $P_{tot} = P_{\mathcal{F}} + P_{\mathcal{R}}$ and the total distance $D_{tot} = d_{\mathcal{F}} + d_{\mathcal{R}}$.

The joint optimization of power allocation and relay locations that minimizes the outage probability subject to sum power and distance constraints is written below

$$\text{Minimize } P_{\text{out}} = \Lambda \left(\frac{\gamma_{th}}{\tilde{\mu}_r}\right)^\delta + \mathcal{G}\left(\frac{\gamma_{th}}{\bar{\gamma}}\right)^{\{K\mu, \frac{2}{\nu}\}}$$

$$\text{s.t. } P_{\mathcal{F}} + P_{\mathcal{R}} \leq P_{tot},$$

$$\text{s.t. } d_{\mathcal{F}} + d_{\mathcal{R}} = D_{tot}, \qquad (44)$$

where

$$\mathcal{G} = \begin{cases} \frac{(\mu(1+\kappa))^{K\mu}}{\left(\frac{\mu\kappa+m}{m}\right)^{Km}(\mu-1)!^K}, & \text{Noise-limited case;} \\ \frac{A_{\mathcal{I}}\left(\frac{\mu\kappa+m}{m\mu(1+\kappa)}\right)^{-\frac{2}{\nu}}}{\Gamma\left(-\frac{2}{\nu}\right)}\Upsilon, & \text{Interference-limited case.} \end{cases}$$

The optimum design of the considered system follows from differentiating the Lagrange cost function $P_{\text{out}} + \Delta(Y_{\mathcal{F}} + Y_{\mathcal{R}} - Y_{tot})$,

where Δ is the Lagrange parameter and $Y \in \{P, d\}$ with respect to the desired parameter P_X, d_X, $X \in \{\mathcal{F}, \mathcal{R}\}$, and solving the obtained equation equated to zero.

A. RELAY POSITIONING UNDER FIXED POWER ALLOCATION

The optimal relay position that minimizes the system outage probability under a predetermined power allocation is the solution of

$$e^{-\delta\delta d_{\mathcal{R}}} - \frac{\theta b e^{-\sigma\delta D_{tot}}\mathcal{G}P_{\mathcal{F}}^\delta}{\sigma\delta\Lambda P_{\mathcal{R}}^b} d_{\mathcal{R}}^{\theta b-1} = 0, \qquad (45)$$

where $b = \{K\mu, \frac{2}{\nu}\}$. Solving the above equation yields the expression for the optimum relay position for general values of θb as

$$d_{\mathcal{R}}^* = \frac{(\theta b - 1)\mathcal{W}\left(\frac{\sigma\delta}{\theta b-1}\left(\frac{\theta b e^{-\sigma\delta D_{tot}}\mathcal{G}P_{\mathcal{F}}^\delta}{\sigma\delta\Lambda P_{\mathcal{R}}^b}\right)^{\frac{1}{1-\theta b}}\right)}{\sigma\delta}, \quad (46)$$

where $\mathcal{W}(\cdot)$ is the principal branch of the Lambert function [56]. When the outage probability performance is dominated by the effect of the path loss of the interference sources (i.e., $b = \frac{2}{\nu}$), then assuming that $\theta = \nu$ (i.e. desired and interfering signals subject to equal path-loss), (46) reduces to

$$d_{\mathcal{R}}^* = \frac{\mathcal{W}\left(\frac{(\sigma\delta)^2 e^{\sigma\delta D_{tot}}\Lambda P_{\mathcal{R}}^{\frac{2}{\nu}}}{2\mathcal{G}P_{\mathcal{F}}^\delta}\right)}{\sigma\delta}, \qquad (47)$$

and $d_{\mathcal{F}}^* = D_{\text{tot}} - d_{\mathcal{R}}^*$.

B. ADAPTIVE POWER ALLOCATION UNDER FIXED RELAY POSITION

The optimum power allocation subject to sum power constraint P_{tot} is obtained from solving the equation stemming from taking the derivative of the Lagrange cost function with respect to $P_{\mathcal{F}}$ and Δ and setting to zero, thereby yielding

$$d_{\mathcal{R}}^{-\frac{\theta b}{b+1}}\left(\frac{\Lambda\delta}{\mathcal{G}b}\right)^{\frac{1}{b+1}} e^{\frac{\sigma\delta d_{\mathcal{F}}}{b+1}} P_{\mathcal{F}}^{\frac{\delta+1}{b+1}} + P_{\mathcal{F}} = P_{tot}. \quad (48)$$

It is hard to find a closed-form expression for the optimal source power. However, a numerical solution can be found by standard iterative root-finding algorithms, such as the Bisection's method and Newton's method. As a special case, when $\delta = b$, we can find the optimal relay power as follows

$$P_{\mathcal{R}}^* = P_{\text{tot}}\left(1 + d_{\mathcal{R}}^{-\frac{\theta b}{b+1}}\left(\frac{\Lambda}{\mathcal{G}}\right)^{\frac{1}{b+1}} e^{\frac{\sigma\delta d_{\mathcal{F}}}{b+1}}\right)^{-1}, \quad (49)$$

and

$$P_{\mathcal{F}}^* = P_{\text{tot}}\left(1 + d_{\mathcal{R}}^{\frac{\theta b}{b+1}}\left(\frac{\mathcal{G}}{\Lambda}\right)^{\frac{1}{b+1}} e^{\frac{-\sigma\delta d_{\mathcal{F}}}{b+1}}\right)^{-1}. \quad (50)$$

From (50), it can be deduced that the optimal power $P_{\mathcal{R}}^*$ increases if (i) the interference level $\bar{\gamma}_I$ (recall here that we

have $A_{\mathcal{I}} = \lambda (\bar{\gamma}_{\mathcal{I}})^{\frac{2}{v}} \Sigma(v)$ in $\mathcal{G}$) affecting the RF users rises, or (ii) the power attenuation due to the distance travelled by the signal is larger for the RF hop compared to the FSO hop.

VI. mmWAVE MULTIUSER MIXED FSO-RF SYSTEMS

The modeling of the mmWave-based links is well-known for LOS wireless backhaul links. The Rician channel model is an appropriate model for near LOS conditions and has been well established for different mmWave-based applications.

Yet, to theoretically obtain the Rician distribution as special case of the κ-μ shadowed fading, we need to set $\mu = 1$ and tend $m \longrightarrow \infty$. However, in practice, the κ-μ shadowed distribution converges rapidly to the Rician distribution, i.e., for $m \approx 15 - 20$ [57].

Noise-limited regime in mmWave networks may happen when most of the interfering sources are susceptible to blockages and obstacles and the received interference power is low enough that the thermal noise is dominant. Alternately, depending on the density of interfering sources, density of the obstacles, and operating beamwidth, mmWave network performance may degrade due to interference (interference-limited regime).

It is quite straightforward to obtain the outage probability and SEP of mmWave multiuser hybrid FSO-RF systems by using the results of section III and IV. In particular, the asymptotic outage probability in mixed FSO/multiuser mmWave networks is obtained from (36) and (38) as

$$P_{out}^{MMv} \overset{(a)}{=} \Lambda \left(\frac{\gamma_{th}}{\widetilde{\mu}_r} \right)^{\min\{\frac{\xi^2}{r}, \frac{L\beta}{r}, \frac{Ln}{r}\}}$$
$$+ \begin{cases} e^{-KK_R} \left(\frac{(1+K_R)\gamma_{th}}{\widetilde{\gamma}} \right)^K, & \mathcal{I}=0; \\ \Upsilon(m \leftarrow \infty) \dfrac{A'_{\mathcal{I}}}{\Gamma(-\frac{2}{v})} \left(\frac{(1+K_R)\gamma_{th}}{\widetilde{\gamma}} \right)^{\frac{2}{v}}, & \mathcal{I}\neq 0. \end{cases}$$
(51)

where $K_R, K_{R_I} > 0$ are the Rice factors of the selected user and interference sources, respectively, and $A'_{\mathcal{I}} = A_{\mathcal{I}}(m_I \rightarrow \infty, \mu_I = 1, \kappa_I = K_{R_I}) = \frac{\lambda(\bar{\gamma}_{\mathcal{I}})^{\frac{2}{v}} \pi \Gamma(1-\frac{2}{v}) e^{-K_{R_I}}}{(1+K_{R_I})^{\frac{2}{v}}} G_{3,2}^{1,1} \left[K_{R_I}^{-1} \Big| \begin{smallmatrix} 1,1,\frac{1}{2} \\ \frac{2}{v},\frac{1}{2} \end{smallmatrix} \right]$. Moreover, (a) follows by letting $\mu = 1$, $\kappa = K_R$ in (38) while applying $\lim_{m \to \infty} \left(1 + \frac{x}{m}\right)^{-m} = e^{-x}$.

Path loss models for mmWave signals have been recently proposed in [64] and [65] inferring that the average received power over the relay-user link is

$$\bar{\gamma} = P_{\mathcal{R}} \left(\frac{\lambda_W}{4\pi d_0} \right)^2 \left(\frac{d_0}{d_{\mathcal{R}}} \right)^{\theta},$$
(52)

where d_0 is a free-space reference distance set to 5 meters in [64], [65], and λ_W stands for the wavelength (7.78 mm in 38 GHz and 10.71 mm in 28 GHz). Moreover, the value of the path-loss exponent θ is equal to 2.2 in 38 GHz and 2.55 in 28 GHz.

VII. NUMERICAL RESULTS

Here we report on various numerical performance results obtained for the outage probability and average SEP expressions derived in Section V for mixed TAPS/user selection AF relaying operating over Málaga-$\mathcal{M}$ and shadowed κ-μ fading channels with cochannel interference. More specifically, we obtained the following results: 1) P_{out} versus SNR/SIR per user (obtained using (16) and (36) in the noise-limited scenario, and (22), and (38) in the presence of PPP distributed interference; see Figs. 2, 3, 4, and 7); 2) The SEP $\mathcal{B}$ versus SNR/SIR per user (obtained using (30), (28) and (42); see Figs. 5 and 6). To validate the accuracy of the aforementioned expressions we compare them with empirically Monte-Carlo simulation performance results.
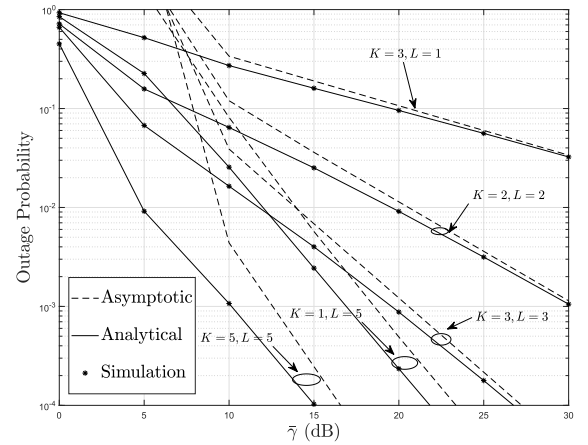

FIGURE 2. The outage probability of noise-limited user selection in mixed Málaga-$\mathcal{M}$/shadowed κ-μ relay networks for different numbers of transmit apertures $L = \{1, 2, 3, 5\}$ and users $K = \{1, 3, 5\}$ when $\gamma_{th} = 5$ dB.

Fig. 2 shows the outage probability for the TAPS/user selection AF relay network in the noise-limited scenario versus the average SNR. The results are calculated for different numbers of transmit FSO apertures $L = \{1, 2, 3, 5\}$ and different numbers of users $K = \{1, 3, 5\}$. In particular, we assume that both users and interferers undergo shadowed κ-μ fading with $m = 3$, $\mu = 1$ and $\kappa = 2$. For the FSO link, the parameters of the Málaga-$\mathcal{M}$ distribution are chosen as $\alpha = 2.5$, $\beta = 1$ and $\xi = 2.1$. We can observe that P_{out} improves with increasing K and/or L. Moreover, the performance evaluation results show that the theoretical outage probability curves are sufficiently close to those obtained by computer simulations and that the asymptotic expansion of P_{out} in (36) is quite tight, particularly at high SNR values.

In Fig. 3, we show the outage performance of interference-limited TAPS/SIR-based user selection versus the average SNR per user for a number of transmit apertures $L = 2$, a number of users $K = 2$, path-loss exponents $v = \{2.3, 3, 4\}$, an INR $\gamma_I = 5$ dB, and $\lambda = 10^{-4}$. We observe very clearly that the outage probability improves with increasing v and that the Monte-Carlo simulation-based curves are in are in
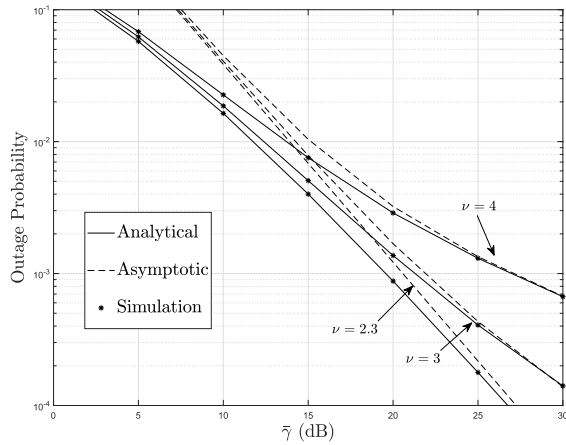
FIGURE 3. The outage probability of mixed FSO/interference-limited multiuser relay networks with selection among $L = 2$ apertures for different various path-loss exponents $\nu = \{2.3, 3, 4\}$.
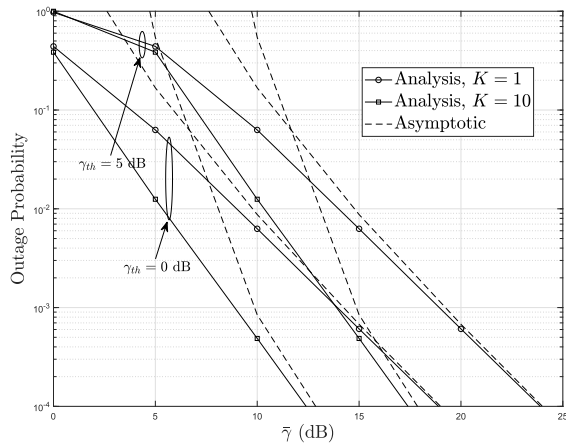

FIGURE 5. The average SEP of noise-limited user selection in mixed Málaga-$\mathcal{M}$/shadowed κ-μ relay networks with $L = K = \{1, 3\}$ and QPSK modulation.

FIGURE 4. The outage probability of noise-limited user selection in mixed Málaga-$\mathcal{M}$/mmWave relay networks for different values of the Rice factor $K_R = \{1, 10\}$ and threshold $\gamma_{th} = \{0, 5\}$ dB.
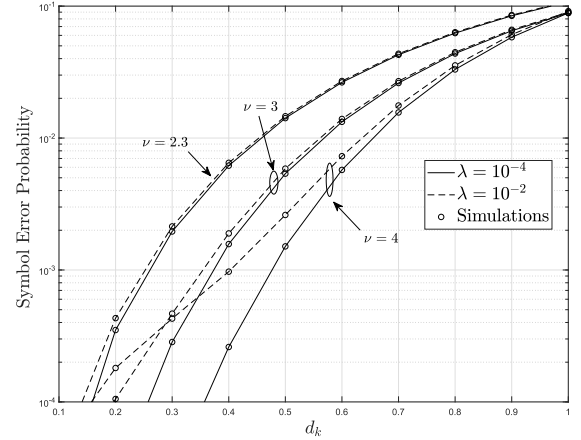
FIGURE 6. The average SEP of mixed Málaga-$\mathcal{M}$/shadowed κ-μ relay networks with the use of TAPS/max-SNR user selection in the presence of PPP interference fields for different path loss exponent $\nu = \{2.3, 3, 4\}$ and intensity of interferers per unit area $\lambda = \{10^{-2}, 10^{-4}\}$ when $L = 2$ and $K = 2$.

excellent agreement with those obtained with our developed analytical results and their associated asymptotic expressions.

Fig. 4 shows the outage probability of a mmWave multiuser AF relay network with aperture selection for a noise-limited scenario versus the average SNR for different values of $\gamma_{th} = \{0, 5\}$ dB. We verify that the analytical curves for the shadowed κ-μ distribution with $\kappa = K_R$, $\mu = 1$ and sufficiently large m set to $m = 15$ for sufficient numerical accuracy perfectly matches those plotted by Monte-Carlo simulations in the Rician case. Furthermore, we observe that a larger γ_{th} increases the outage probability.

Fig. 5 depicts the average SEP performance of mixed TAPS/user selection relay systems in Málaga-$\mathcal{M}$ and shadowed κ-μ fading channels both for $L = K = \{1, 3\}$. In the legend, we have identified some particular turbulence and fading distribution cases that simply stem from the general Málaga and κ-μ shadowed fading scenarios, respectively. In particular, when $g = 0$ and $\phi = 1$, (28) reduces to the SEP for Gamma-Gamma ($\mathcal{G}$-$\mathcal{G}$) TAPS/SNR-based selection over shadowed κ-μ fading. The latter, includes as special cases
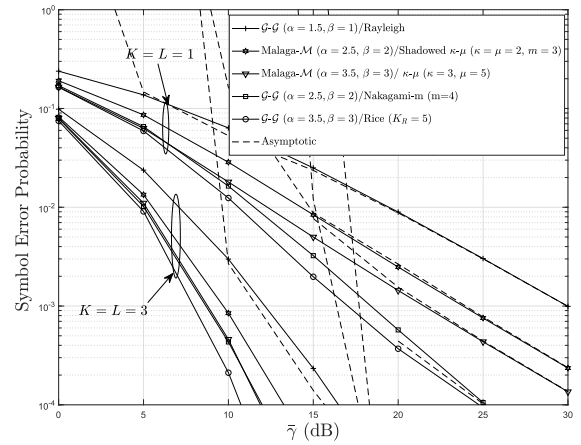
κ-μ ($m \to \infty$), Nakagami-m ($\mu = m$ and $\kappa \to 0$), Rayleigh ($\mu = m = 1$ and $\kappa \to 0$), and Rice ($\mu = 1, \kappa = K$ and $m \to \infty$), to name a few [54, Table I]. The exact match with Monte-Carlo simulation results confirms the precision of our theoretical analysis. Moreover, we notice that the exact and asymptotic expansion in (30) and (42), respectively, agree very well at high SNRs.

Fig. 6 presents the average SEP performance of interference-limited user selection with identical PPP interference versus the distance between the relay and the macrocell users d_k. We plot the error rate for different path-loss exponent values $\nu = \{2.3, 3, 4\}$ when the number of transmit apertures $L = 2$ and the number of users $K = 2$, the average INR is of 5 dB and modulation scheme is QPSK. We observe that the error probability increases when the distance d_k increases, while it deceases when the path-loss exponent increases. Moreover, the error probability significantly degrades with an increasing density of interferers per unit area.
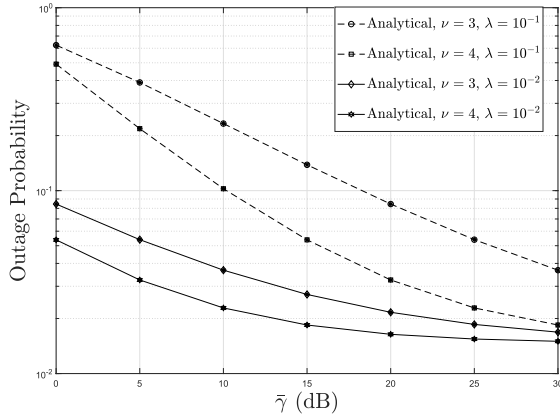
FIGURE 7. The outage probability of mixed Málaga-$\mathcal{M}$/shadowed κ-μ relay networks with the use of TAPS/max-SNR user selection for different PPP interference profiles when $L = K = 5$.
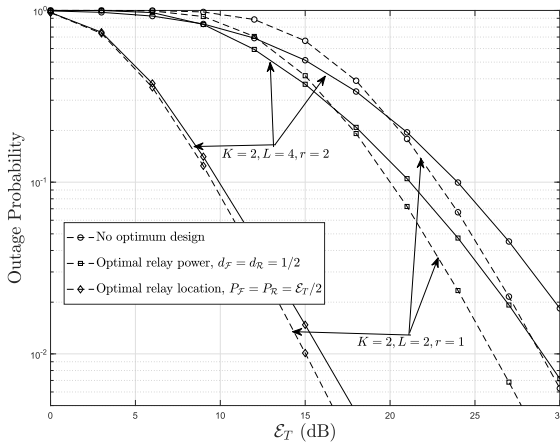

FIGURE 8. The outage probability for different power/positions allocations with TAPS/max-SNR user selection when $k = 2$, $L = \{2, 4\}$, and $r = \{1, 2\}$.

Fig. 7 depicts the outage probability of TAPS/SNR-based user selection versus the average per user SNR over shadowed κ-μ fading with $m = 3$, $\mu = 1$ and $\kappa = 5$ under the same power level of interference among users with $\bar{\gamma}_I = 5$ dB. We assume a fixed average electrical SNR of the FSO link of $\widetilde{\mu}_r = 10$ dB and strong turbulence conditions (i.e., with $\beta = 1$, $\alpha = 2.5$) and IM/DD detection (i.e., with $r = 2$). The analytical results illustrate the outage expression derived in (22). In fact, the system saturates as the average transmitted power over the first hop is constant. The limitation is mainly observed by the creation of the outage floor that substantially degrades the system performance. The degradation caused by increasing the number of interferers or path loss exponent is confirmed again and both analytical and simulation curves show a quasi-perfect match.

Fig. 8 shows the impact of power/position allocations on the outage probability of SNR-based user selection in a mixed TAPS FSO/multiuser AF relay system against $P_{tot} = \mathcal{E}_T$ dB when $\gamma_{th} = 0$ dB, $\kappa = 5$, $\mu = 1$, $m = 2$, $\alpha = 2.5$, $\beta = 1$, and $\xi = 3.5$. Moreover, we investigate the impact of the

proposed power/position allocation formula in (46) and (50) on the outage performance and compare then to the case of no power allocation. We observe that the benefits of optimizing the relay position outperforms those of optimizing power allocation.

VIII. CONCLUSION

We presented in this contribution new formulated problems that integrate different processing designs and network conditions in mixed FSO-RF relay networks. We also considered a very generic two-hop propagation model over Málaga-$\mathcal{M}$ optical channels with pointing errors on the first hop and shadowed κ-μ distributed radio channels that account both for LOS and NLOS scenarios on the second hop in the presence of Poisson field interference. First of all, we analyzed the performance of mixed FSO-RF control-access schemes for multiuser networks using TAPS/max-SNR user selection. We also developed, new analytical results for some key performance metrics, namely, the outage probability and the average SEP under PPP interference, then obtained their asymptotic approximations from which we have been to characterize key performance indicators, such as the diversity and coding gains. We were then able to extend our treatment to cover the compelling case of mmWave user selection made possible owing the suitability of the shadowed κ-μ distribution in modeling LOS channels. Under weak atmospheric turbulence conditions, we showed that the system is dominated in performance by the RF channels and achieves a full diversity order of $K\mu$ and $\frac{2}{\nu}$ in in noise-limited and PPP interference-limited scenarios, respectively. Whereas, its performance is dominated under severe atmospheric turbulence conditions by the FSO channel and its diversity order is proportional to the minimum value of L times the turbulence fading parameters and the pointing errors parameter. we showed that the proposed power and position allocation formulas improve significantly the outage performance.

APPENDIX A
CALCULATION OF $F_{\gamma_\mathcal{R}}^{(c)}(\gamma)$
For the outage probability expression in (15), the ccdf of $\gamma_\mathcal{R}$ can be expressed as

$$F_{\gamma_\mathcal{R}}^{(c)}(\gamma) = Pr\left(\frac{\gamma_b}{\mathcal{I}} \geq \gamma\right)$$
$$= \int_0^\infty F_{\gamma_b}^{(c)}(\gamma y) f_\mathcal{I}(y) dy, \qquad (53)$$

where $f_\mathcal{I}(y) = \mathcal{L}^{-1}\{\psi_\mathcal{I}(z), y\}$ and $\psi_\mathcal{I}(z) = \exp\left[-\lambda\left(\bar{\gamma}_\mathcal{I}z\right)^{\frac{2}{\nu}}\Sigma(\nu)\right] = \mathcal{H}_{0,1}^{1,0}\left[\lambda\left(\bar{\gamma}_\mathcal{I}z\right)^{\frac{2}{\nu}}\Sigma(\nu)\Big|_{(0,\ 1)}^{-}\right]$, under identical interference on users $\mathcal{I}_{k^*} = \mathcal{I}$, for $k = 1, \ldots, K$ with average power $\bar{\gamma}_\mathcal{I}$. Now the ccdf of γ_b defined as the post-user selection SNR is obtained in (5). Inserting the latter into (53) then applying the binomial expansion and

averaging over the distribution of $\mathcal{I}$ yields

$$F_{\gamma_{\mathcal{R}}}^{(c)}(\gamma) = \sum_{\mathcal{S}\setminus\varnothing}\sum_{\mathcal{J}}\sum_{\mathcal{R}}(-1)^{Q-1}C_{\mathcal{S},\mathcal{J},\mathcal{R}}\gamma^{r_{\mathcal{J},\mathcal{R}}}e^{-E_{\mathcal{S},\mathcal{J}}\gamma}\mathcal{J},$$

(54)

where

$$\mathcal{J} = \mathbb{E}_y\left[\mathcal{I}^{r_{\mathcal{J},\mathcal{R}}}\,e^{-E_{\mathcal{S},\mathcal{J}}\mathcal{I}\gamma}\right]$$
$$\overset{(a)}{=} (-1)^{r_{\mathcal{J},\mathcal{R}}}\left[\frac{d^{r_{\mathcal{J},\mathcal{R}}}\psi_{\mathcal{I}}(z)}{dz^{r_{\mathcal{J},\mathcal{R}}}}\right]\Big|_{z=E_{\mathcal{S},\mathcal{J}}\gamma}$$
$$\overset{(b)}{=} \frac{(-1)^{r_{\mathcal{J},\mathcal{R}}}}{(E_{\mathcal{S},\mathcal{J}}\gamma)^{r_{\mathcal{J},\mathcal{R}}}}\mathcal{H}_{1,2}^{2,0}\left[A_{\mathcal{I}}(E_{\mathcal{S},\mathcal{J}}\gamma)^{\frac{2}{\nu}}\left|\begin{matrix}(0,\frac{2}{\nu})\\(r_{\mathcal{J},\mathcal{R}},\frac{2}{\nu}),(0,1)\end{matrix}\right.\right],$$

(55)

where $A_{\mathcal{I}} = \lambda\,(\bar{\gamma}_{\mathcal{I}})^{\frac{2}{\nu}}\,\Sigma(\nu)$, (a) follows from the Laplace transform property [58, Eq. (1.1.2.9)], and (b) follows from the derivative property of the Fox's H-function [58, Eq. (2.2.2)]. Using (55) we obtain the ccdf expression in (18) which entails an insolvable integral of shifted Fox's H functions, if plugged into (15). Therefore, for sake of tractability, $\mathcal{J}$ can be further expanded as

$$\mathcal{J} \overset{(c)}{=} (-1)^{r_{\mathcal{J},\mathcal{R}}}e^{-A_{\mathcal{I}}z^{\frac{2}{\nu}}}\sum_{k=0}^{r_{\mathcal{J},\mathcal{R}}}\Phi_k(-A_{\mathcal{I}}z^{\frac{2}{\nu}})^k]\,|_{z=E_{\mathcal{S},\mathcal{J}}\gamma},\quad (56)$$

where $\Phi_k = \sum_{i=1}^{k}\frac{(-1)^i\left(\frac{2}{\nu}k-\frac{2}{\nu}i-r_{\mathcal{J},\mathcal{R}}\right)_{r_{\mathcal{J},\mathcal{R}}}}{i!(k-i)!}$ with $(a)_n$ being the Pochhammer symbol [56], and (c) follows from the differentiation of the exponential function. Using the Taylor series expansion of the exponential, and after some mathematical manipulations, we obtain

$$\mathcal{J} = (-1)^{r_{\mathcal{J},\mathcal{R}}}(E_{\mathcal{S},\mathcal{J}}\gamma)^{-r_{\mathcal{J},\mathcal{R}}}$$
$$\times \sum_{j=0}^{\infty}\sum_{k=0}^{r_{\mathcal{J},\mathcal{R}}}\frac{(-1)^{k+j}\Phi_k}{j!}(E_{\mathcal{S},\mathcal{J}}\gamma)^{\frac{2}{\nu}(k+j)}(A_{\mathcal{I}})^{k+j}.\quad (57)$$

Inserting (57) into (54) yields (19), and this concludes the proof.

APPENDIX B
ASYMPTOTIC $F_{\gamma_{\mathcal{X}}}$, $\mathcal{X}\in\{\mathcal{F},\mathcal{R}\}$

The asymptotic performance of a dual-hop relaying system depends on the behavior of $f_{\gamma_X}(y)$, $X\in\{\mathcal{F},\mathcal{X}\}$ at $y=0_+$. Assume that $f_{\gamma_X}(y)$ accepts a Taylor series expansion at $y\to0_+$ as $f_{\gamma_X}(y)\underset{y\to0_+}{\approx}a_Xy^{b_X}+o(y^{b_X})$, where a_X and b_X are appropriate constants. Then the corresponding per hop cdf can be approximated as $F_{\gamma_X}(y)\underset{y\to0_+}{\approx}a_X/(b_x+1)y^{b_x+1}+o(y^{b_X})$.

A. CALCULATION OF $F_{\gamma_{\mathcal{F}}}^{\infty}(\gamma)$

Before delving in the asymptotic expansion of the first-hop FSO TAPS cdf, it is more convenient to reexpress $F_{\gamma_{\mathcal{F}}}$ in (12)

as follows

$$F_{\gamma_{\mathcal{F}}}(\gamma) = 1 - 2\xi^2\sum_{p=1}^{L}(-1)^{p-1}(A\sqrt{\pi})^p\widetilde{\sum_k}\widetilde{\sum_i}\widetilde{\sum_j}\prod_{t=1}^{p}$$

$$\times \frac{2^{j_t}\Psi_{k_t,i_t}}{B^{\alpha+k_t-j_t}}\frac{\Gamma(\alpha+k_t-i_t-\frac{1}{2})}{j_t!}(2Bp)^{(2\xi^2-\sum_{t=1}^{p}j_t)}$$

$$\times \left(\frac{\gamma}{\widetilde{\mu}_r}\right)^{\frac{\xi^2}{r}}\Gamma\left(\sum_{t=1}^{p}j_t-2\xi^2, 2Bp\sqrt{\left(\frac{\gamma}{\widetilde{\mu}_r}\right)^{\frac{1}{r}}}\right),$$

(58)

where $B = \sqrt{\frac{\alpha\beta}{g\beta+\phi}}$, $\widetilde{\sum_k} = \sum_{k_1}^{\beta}\cdots\sum_{k_p}^{\beta}$, $\widetilde{\sum_i} = \sum_{i_1}^{\alpha-k_1-\frac{1}{2}}\cdots\sum_{i_p}^{\alpha-k_p-\frac{1}{2}}$, and $\widetilde{\sum_j} = \sum_{j_1}^{\alpha+k_1-i_1-\frac{3}{2}}\cdots\sum_{j_p}^{\alpha+k_p-i_p-\frac{3}{2}}$. For large values of $\widetilde{\mu}_r$ it holds that $\Gamma(a,z)\underset{z\to0}{\approx}\Gamma(a)-\frac{z^a}{a}$. Then keeping in mind that $K_{-\nu}(z)\underset{\nu\notin\mathbb{Z}}{=}K_{\nu}(z)$ in (8), the asymptotic expansion of the FSO TAPS SNR corresponding to its pdf series expansion from (58) is obtained as

$$F_{\gamma_{\mathcal{F}}}(\gamma)\underset{\widetilde{\mu}_r\to\infty}{\simeq}\Lambda\left(\frac{\gamma}{\widetilde{\mu}_r}\right)^{\min\left(\frac{\xi^2}{r},\frac{L\beta}{r},\frac{Ln}{r}\right)},\quad (59)$$

where

$$\frac{\Lambda}{\xi^2} = \begin{cases} 2\sum_{p=1}^{L}(-A\sqrt{\pi})^p(2\,Bp)^{2\xi^2}\widetilde{\sum_k}\widetilde{\sum_i}\widetilde{\sum_j}\Xi_1, \\ \qquad\qquad\qquad\qquad \delta = \frac{\xi^2}{r}; \\ \left(\frac{A\sqrt{\pi}2^{2\beta-1}\psi_{\beta,\alpha-\beta-\frac{1}{2}}}{B^{\alpha-\beta}(\xi^2-\beta)}\right)^L, \\ \qquad\qquad\qquad\qquad \delta = \frac{L\beta}{r}; \\ \left(\frac{A\sqrt{\pi}2^{2\alpha-1}\psi_{\beta,\beta-\alpha-\frac{1}{2}}}{B^{\alpha-\beta}(\xi^2-\alpha)}\right)^L, \\ \qquad\qquad\qquad\qquad \delta = \frac{L\alpha}{r}. \end{cases}$$

(60)

with $\Xi_1 = \prod_{t=1}^{p}\frac{\Psi_{k_t,i_t}\Gamma(\alpha+k_t-i_t-\frac{1}{2})}{B^{\alpha+k_t}p^{i_t}j_t!}\Gamma\left(\sum_{t=1}^{p}j_t-2\xi^2\right)$ and $\delta = \min\left(\frac{\xi^2}{r},\frac{L\beta}{r},\frac{L\alpha}{r}\right)$.

B. CALCULATION OF $F_{\gamma_{\mathcal{R}}}^{\infty}(\gamma)$

In the RF side, the users are assumed to have identical channels i.e., $N_k = N$ and the set of parameters $\{C_{j,k}, m_{j,k}, \Omega_{j,k}\} = \{C_j, m_j, \Omega_j\}$ for $k = 1\ldots K$. Moreover, when $\mu\leq m$, we have

$$\Omega_j = \Omega = \frac{\mu\kappa+m}{m}\frac{\bar{\gamma}}{\mu(1+\kappa)},\quad j = 1,\ldots,N \quad (61)$$

with $\bar{\gamma}$ being the average SNR.

1) NOISE-LIMITED SCENARIO

After applying the Taylor series expansion of exponentials ($e^{-x} \approx 1 - x$ as $x \to 0$), the cdf in (4) simplifies when $m \geq \mu$ to

$$F_{\gamma_b}(\gamma) \overset{(a)}{\simeq} \left(\sum_{j=0}^{m-\mu} \frac{C_j}{(m-j-1)!} \left(\frac{\gamma}{\Omega} \right)^{m-j} \right)^K$$

$$\underset{\bar{\gamma} \to \infty}{\simeq} \left(\frac{C_{m-\mu}}{(\mu-1)!} \right)^K \left(\frac{\gamma}{\Omega} \right)^{K\mu}, \quad (62)$$

where (a) follows after recognizing that $\sum_{j=0}^{m-\mu} C_j = 1$ with $C_i = \binom{m-\mu}{i} \left(\frac{\mu\kappa + m}{m} \right)^{-i} \left(\frac{\mu\kappa + m}{\mu\kappa} \right)^{m-\mu-i}$.

2) INTERFERENCE-LIMITED SCENARIO

In this case, the asymptotic cdf of the RF SIR depends on the behavior of $f_{\gamma_{\mathcal{R}}}(y)$, given in (6) at $y = 0_+$. Then, differentiating (6) over γ yields

$$f_{\gamma_{\mathcal{R}}}(\gamma) = \frac{d}{d\gamma} \left\{ 1 - \sum_{\mathcal{S}\backslash\varnothing} \sum_{\mathcal{J}} \sum_{\mathcal{R}} \Pi_{\mathcal{SJR}} \right.$$

$$\left. \times \mathcal{H}_{1,2}^{2,0} \left[A_{\mathcal{I}} (E_{\mathcal{SJ}}\gamma)^{\frac{2}{\nu}} \left| \begin{matrix} (0, \frac{2}{\nu}) \\ (r_{\mathcal{J},\mathcal{R}}, \frac{2}{\nu}), (0, 1) \end{matrix} \right. \right] \right\}$$

$$= -\gamma^{-1} \sum_{\mathcal{S}\backslash\varnothing} \sum_{\mathcal{J}} \sum_{\mathcal{R}} \Pi_{\mathcal{SJR}}$$

$$\times \mathcal{H}_{2,3}^{2,1} \left[A_{\mathcal{I}} (E_{\mathcal{SJ}}\gamma)^{\frac{2}{\nu}} \left| \begin{matrix} (0, \frac{2}{\nu}), (0, \frac{2}{\nu}) \\ (r_{\mathcal{J},\mathcal{R}}, \frac{2}{\nu}), (0, 1), (1, \frac{2}{\nu}) \end{matrix} \right. \right]. \quad (63)$$

Using the identities $\Gamma\left(1 - \frac{2}{\nu}s\right) = -\frac{2}{\nu}S\Gamma\left(\frac{2}{\nu}S\right)$ and $\Gamma(1 + \frac{2}{\nu}s) = \frac{2}{\nu}S\Gamma\left(\frac{2}{\nu}s\right)$ along with the definition of the Fox's H-function [58, Eq. (1.2)], $f_{\gamma_{\mathcal{R}}}(\gamma)$ can be written as

$$f_{\gamma_{\mathcal{R}}}(\gamma) = \gamma^{-1} \sum_{\mathcal{S}\backslash\varnothing} \sum_{\mathcal{J}} \sum_{\mathcal{R}} \Pi_{\mathcal{SJR}}$$

$$\times \mathcal{H}_{1,2}^{2,0} \left[A_{\mathcal{I}} (E_{\mathcal{SJ}}\gamma)^{\frac{2}{\nu}} \left| \begin{matrix} (0, \frac{2}{\nu}) \\ (r_{\mathcal{J},\mathcal{R}}, \frac{2}{\nu}), (0, 1) \end{matrix} \right. \right]. \quad (64)$$

The above pdf can be expanded as

$$f_{\gamma_{\mathcal{R}}}(y) = \frac{\Delta_t}{\gamma} \mathcal{H}_{1,2}^{2,0} \left[A_{\mathcal{I}} \left(\frac{p\gamma}{\Omega} \right)^{\frac{2}{\nu}} \left| \begin{matrix} (0, \frac{2}{\nu}) \\ (r_{\mathcal{J},\mathcal{R}}, \frac{2}{\nu}), (0, 1) \end{matrix} \right. \right], \quad (65)$$

where

$$\Delta_t = \sum_{p=1}^{K} \binom{K}{p} (-1)^p \sum_{j_1=0}^{m-\mu} \cdots \sum_{j_p=0}^{m-\mu} \sum_{r_1=1}^{m_{j_1}} \cdots \sum_{r_p=1}^{m_{j_p}} \prod_{n=1}^{p} \left(\frac{C_{j_n}}{r_n! p^{r_n}} \right). \quad (66)$$

Recall that the Fox's H-function has the following power series expansion [66, Eq. (1.3.7)]:

$$\mathcal{H}_{p,q}^{m,n} \left[x \left| \begin{matrix} (a_p, A_p) \\ (b_q, B_q) \end{matrix} \right. \right] = \sum_{j=1}^{m} \sum_{l=0}^{\infty} h_{jl}^* x^{\frac{b_j+l}{B_j}}, \quad (67)$$

where the constants h_{jl}^* are given by [66, Eq. (1.3.6)]

$$h_{jl}^* = \frac{(-1)^l \prod_{i=1, i \neq j}^{m} \Gamma\left(b_i - [b_j + l]\frac{B_i}{B_j}\right)}{l! B_j \prod_{i=n+1}^{p} \Gamma\left(a_i - [b_j + l]\frac{A_i}{B_j}\right)}$$

$$\times \frac{\prod_{i=1}^{n} \Gamma\left(1 - a_i + [b_j + l]\frac{A_i}{B_j}\right)}{\prod_{i=m+1}^{q} \Gamma\left(1 - b_i + [b_j + l]\frac{B_i}{B_j}\right)}. \quad (68)$$

Then keeping only the first two terms in the series expansion of $f_{\gamma_{\mathcal{R}}}(\gamma)$, we show that

$$F_{\gamma_{\mathcal{R}}}(\gamma) \underset{\bar{\gamma} \to \infty}{\simeq} \Delta_t$$

$$\begin{cases} \dfrac{\nu}{2} \dfrac{\Gamma(-r_{sum}\frac{\nu}{2})}{\Gamma(-r_{sum})} A_{\mathcal{I}}^{\frac{r_{sum}\nu}{2}} \left(\dfrac{p\gamma}{\Omega} \right)^{r_{sum}}, \\ \qquad\qquad \text{if } \dfrac{2}{\nu} > r_{sum}; \\ -\dfrac{\Gamma(r_{sum} - \frac{2}{\nu})}{\Gamma(-\frac{2}{\nu})} A_{\mathcal{I}} \left(\dfrac{p\gamma}{\Omega} \right)^{\frac{2}{\nu}}, \\ \qquad\qquad \text{if } \dfrac{2}{\nu} < r_{sum}, \end{cases} \quad (69)$$

where $r_{sum} = \sum_{p=1}^{K} r_p$. From (69), it is evident that the diversity order of the considered system is determined either by $K\mu$ or by $\frac{2}{\nu}$ and is equal to $\min\{\frac{2}{\nu}, K\mu\}$. However, since $K\mu > 1$ as we assume only integer values of μ, the diversity order is determined by $\frac{2}{\nu}$ and decreases as ν increases.

REFERENCES

[1] N. D. Chatzidiamantis, H. G. Sandalidis, G. K. Karagiannidis, and M. Matthaiou, "Inverse Gaussian modeling of turbulence-induced fading in free-space optical systems," *J. Lightw. Technol.*, vol. 29, no. 10, pp. 1590–1596, May 15, 2011.

[2] J. N. Laneman, D. N. C. Tse, and G. W. Wornell, "Cooperative diversity in wireless networks: Efficient protocols and outage behavior," *IEEE Trans. Inf. Theory*, vol. 50, no. 12, pp. 3062–3080, Dec. 2004.

[3] E. Lee, J. Park, D. Han, and G. Yoon, "Performance analysis of the asymmetric dual-hop relay transmission with mixed RF/FSO links," *IEEE Photon. Technol. Lett.*, vol. 23, no. 21, pp. 1642–1644, Nov. 1, 2011.

[4] I. S. Ansari, F. Yilmaz, and M.-S. Alouini, "Impact of pointing errors on the performance of mixed RF/FSO dual-hop transmission systems," *IEEE Wireless Commun. Lett.*, vol. 2, no. 3, pp. 351–354, Jun. 2013.

[5] A. Jurado-Navas, J. M. Garrido-Balsells, J. F. Paris, M. Castillo-Vázquez, and A. Puerta-Notario, "Impact of pointing errors on the performance of generalized atmospheric optical channels," *Opt. Express*, vol. 20, no. 11, pp. 12550–12562, May 2012.

[6] N. Saquib, M. S. R. Sakib, A. Saha, and M. Hussain, "Free space optical connectivity for last mile solution in Bangladesh," in *Proc. 2nd Int. Conf. Educ. Technol. Comput.*, Shanghai, China, Jun. 2010, pp. 484–487.

[7] E. Zedini, I. S. Ansari, and M.-S. Alouini, "Performance analysis of mixed Nakagami-$\mathcal{M}$ and Gamma–Gamma dual-hop FSO transmission systems," *IEEE Photon. J.*, vol. 7, no. 1, Feb. 2015, Art. no. 7900120.

[8] S. Anees and M. R. Bhatnagar, "Performance of an amplify-and-forward dual-hop asymmetric RF–FSO communication system," *J. Opt. Commun. Netw.*, vol. 7, no. 2, pp. 124–135, Feb. 2015.

[9] G. T. Djordjevic, M. I. Petkovic, A. M. Cvetkovic, and G. K. Karagiannidis, "Mixed RF/FSO relaying with outdated channel state information," *IEEE J. Sel. Areas Commun.*, vol. 33, no. 9, pp. 1935–1948, Sep. 2015.

[10] J. Zhang, L. Dai, Y. Zhang, and Z. Wang, "Unified performance analysis of mixed radio frequency/free-space optical dual-hop transmission systems," *J. Lightw. Technol.*, vol. 33, no. 11, pp. 2286–2293, Jun. 1, 2015.

[11] L. Kong, W. Xu, L. Hanzo, H. Zhang, and C. Zhao, "Performance of a free-space-optical relay-assisted hybrid RF/FSO system in generalized *M*-distributed channels," *IEEE Photon. J.*, vol. 7, no. 5, Oct. 2015, Art. no. 7903319.

[12] E. Soleimani-Nasab and M. Uysal, "Generalized performance analysis of mixed RF/FSO cooperative systems," *IEEE Trans. Wireless Commun.*, vol. 15, no. 1, pp. 714–727, Jan. 2016.

[13] P. V. Trinh, T. C. Thang, and A. T. Pham, "Mixed mmWave RF/FSO relaying systems over generalized fading channels with pointing errors," *IEEE Photon. J.*, vol. 9, no. 1, Feb. 2017, Art. no. 5500414.

[14] M. Hajji and F. El Bouanani, "Performance analysis of mixed weibull and Gamma-Gamma dual-hop RF/FSO transmission systems," in *Proc. Int. Conf. Wireless Netw. Mobile Commun.*, Rabat, Morocco, Nov. 2017, pp. 1–5.

[15] F. Babich and G. Lombardi, "Statistical analysis and characterization of the indoor propagation channel," *IEEE Trans. Commun.*, vol. 48, no. 3, pp. 455–464, Mar. 2000.

[16] A. Soulimani and M. Benjillali, "Closed-form performance analysis of generalized M-QAM over multihop weibull fading channels," in *Proc. Int. Conf. Wireless Netw. Mobile Commun.*, Marrakech, Morocco, Oct. 2015, pp. 1–5.

[17] S. L. Cotton, "Human body shadowing in cellular device-to-device communications: Channel modeling using the shadowed κ-μ fading model," *IEEE J. Sel. Areas Commun.*, vol. 33, no. 1, pp. 111–119, Jan. 2015.

[18] I. Trigui, N. Cherif, and S. Affes, "Relay-assisted mixed FSO/RF systems over Málaga-$\mathcal{M}$ and κ-μ shadowed fading channels," *IEEE Wireless Commun. Lett.*, vol. 6, no. 5, pp. 682–685, Oct. 2017.

[19] H. Lei, Z. Dai, I. S. Ansari, K.-H. Park, G. Pan, and M.-S. Alouini, "On secrecy performance of mixed RF-FSO systems," *IEEE Photon. J.*, vol. 9, no. 4, Aug. 2017, Art. no. 7904814.

[20] H. Arezumand, H. Zamiri-Jafarian, and E. Soleimani-Nasab, "Outage and diversity analysis of underlay cognitive mixed RF-FSO cooperative systems," *J. Opt. Commun. Netw.*, vol. 9, no. 10, pp. 909–920, Oct. 2017.

[21] I. Trigui, N. Cherif, S. Affes, X. Wang, V. Leung, and A. Stephenne, "Interference-limited mixed Málaga-$\mathcal{M}$ and Generalized-K dual-hop FSO-RF systems," in *Proc. IEEE 28th Annu. Int. Symp. Pers., Indoor, Mobile Radio Commun.*, Montreal, QC, Canada, Oct. 2017, pp. 1–6.

[22] L. Yang, M. O. Hasna, and X. Gao, "Performance of mixed RF/FSO with variable gain over generalized atmospheric turbulence channels," *IEEE J. Sel. Areas Commun.*, vol. 33, no. 9, pp. 1913–1924, Sep. 2015.

[23] N. Sharma, A. Bansal, and P. Garg, "Decode-and-forward relaying in mixed η-μ and gamma–gamma dual hop transmission system," *IET Commun.*, vol. 10, no. 14, pp. 1769–1776, 2016.

[24] J. Gupta, V. K. Dwivedi, and V. Karwal, "On the performance of RF-FSO system over Rayleigh and Kappa-Mu/Inverse Gaussian fading environment," *IEEE Access*, vol. 6, pp. 4186–4198, 2018.

[25] O. M. S. Al-Ebraheemy, A. M. Salhab, A. Chaaban, S. A. Zummo, and M. Alouini, "Precise outage analysis of mixed RF/unified-FSO DF Relaying with HD and 2 IM-DD channel models," in *Proc. 13th Int. Wireless Commun. Mobile Comput. Conf.*, Valencia, Spain, Jun. 2017, pp. 1184–1189.

[26] N. Singhal, A. Bansal, and A. Kumar, "Performance evaluation of decode-and-forward-based asymmetric SIMO-RF/FSO system with misalignment errors," *IET Commun.*, vol. 11, no. 14, pp. 2244–2252, 2017.

[27] N. Varshney and A. K. Jagannatham, "Cognitive decode-and-forward MIMO-RF/FSO cooperative relay networks," *IEEE Commun. Lett.*, vol. 21, no. 4, pp. 893–896, Apr. 2017.

[28] N. Varshney and P. Puri, "Performance analysis of decode-and-forward-based mixed MIMO-RF/FSO cooperative systems with source mobility and imperfect CSI," *J. Lightw. Technol.*, vol. 35, no. 11, pp. 2070–2077, Jun. 1, 2017.

[29] B. T. Vu, T. C. Thang, and A. T. Pham, "Selective relay decode-and-forward QAM/FSO systems over atmospheric turbulence channels," in *Proc. 9th Int. Symp. Commun. Syst., Netw. Digit. Sign*, Manchester, U.K., Jul. 2014, pp. 407–410.

[30] S. I. Hussain, M. M. Abdallah, and K. A. Qaraqe, "Power optimization and kth order selective relaying in free space optical networks," in *Proc. 7th IEEE GCC Conf. Exhib.*, Doha, Qatar, Nov. 2013, pp. 330–333.

[31] C. Abou-Rjeily, "Performance analysis of selective relaying in cooperative free-space optical systems," *J. Lightw. Technol.*, vol. 31, no. 18, pp. 2965–2973, Sep. 15, 2013.

[32] N. D. Chatzidiamantis and G. K. Karagiannidis, "On the distribution of the sum of gamma-gamma variates and applications in RF and optical wireless communications," *IEEE Trans. Commun.*, vol. 59, no. 5, pp. 1298–1308, May 2011.

[33] J.-Y. Wang, J.-B. Wang, M. Chen, and X. Song, "Performance analysis for free-space optical communications using parallel all-optical relays over composite channels," *IET Commun.*, vol. 8, no. 9, pp. 1437–1446, Jun. 2014. doi: 10.1049/iet-com.2013.0754.

[34] M. I. Petkovic, A. M. Cvetkovic, G. T. Djordjevic, and G. K. Karagiannidis, "Partial relay selection with outdated channel state estimation in mixed RF/FSO systems," *J. Lightw. Technol.*, vol. 33, no. 13, pp. 2860–2867, Jul. 1, 2015.

[35] S. Enayati and H. Saeedi, "Deployment of hybrid FSO/RF links in backhaul of relay-based rural area cellular networks: Advantages and performance analysis," *IEEE Commun. Lett.*, vol. 20, no. 9, pp. 1824–1827, Sep. 2016.

[36] M. Najafi, V. Jamali, and R. Schober, "Optimal relay selection for the parallel hybrid RF/FSO relay channel: Non-buffer-aided and buffer-aided designs," *IEEE Trans. Commun.*, vol. 65, no. 7, pp. 2794–2810, Jul. 2017.

[37] C. Abou-Rjeily, "Performance analysis of up-link and down-link mixed RF/FSO links with multiple relays," in *Proc. 25th Int. Conf. Softw., Telecommun. Comput. Netw.*, Split, Croatia, Sep. 2017, pp. 1–6.

[38] E. Balti, M. Guizani, B. Hamdaoui, and B. Khalfi, "Aggregate hardware impairments over mixed RF/FSO relaying systems with outdated CSI," *IEEE Trans. Commun.*, vol. 66, no. 3, pp. 1110–1123, Mar. 2018.

[39] E. Balti and M. Guizani, "Mixed RF/FSO cooperative relaying systems with co-channel interference," *IEEE Trans. Commun.*, vol. 66, no. 9, pp. 4014–4027, Sep. 2018. doi: 10.1109/TCOMM.2018.2818697.

[40] N. I. Miridakis, M. Matthaiou, and G. K. Karagiannidis, "Multiuser relaying over mixed RF/FSO links," *IEEE Trans. Commun.*, vol. 62, no. 5, pp. 1634–1645, May 2014.

[41] V. Jamali, D. S. Michalopoulos, M. Uysal, and R. Schober, "Mixed RF and hybrid RF/FSO relaying," in *Proc. IEEE Global Commun. Conf.*, San Diego, CA, USA, Dec. 2015, pp. 1–6.

[42] B. Makki, T. Svensson, T. Eriksson, and M.-S. Alouini, "On the performance of HARQ-based RF-FSO links," in *Proc. IEEE Global Commun. Conf.*, San Diego, CA, USA, Dec. 2015, pp. 1–7.

[43] B. Makki, T. Svensson, T. Eriksson, and M.-S. Alouini, "On the performance of RF-FSO links with and without hybrid ARQ," *IEEE Trans. Wireless Commun.*, vol. 15, no. 7, pp. 4928–4943, Jul. 2016.

[44] E. Zedini, H. Soury, and M.-S. Alouini, "On the performance analysis of dual-hop mixed FSO/RF systems," *IEEE Trans. Wireless Commun.*, vol. 15, no. 5, pp. 3679–3689, May 2016.

[45] A. M. Salhab, F. S. Al-Qahtani, R. M. Radaydeh, S. A. Zummo, and H. Alnuweiri, "Power allocation and performance of multiuser mixed RF/FSO relay networks with opportunistic scheduling and outdated channel information," *J. Lightw. Technol.*, vol. 34, no. 13, pp. 3259–3272, Jul. 1, 2016.

[46] A. M. Salhab, "Performance of multiuser mixed RF/FSO relay networks with generalized order user scheduling and outdated channel information," *Arabian J. Sci. Eng.*, vol. 40, no. 9, pp. 2671–2683, Jul. 2015.

[47] A. H. A. El-Malek, A. M. Salhab, S. A. Zummo, and M.-S. Alouini, "Security-reliability trade-off analysis for multiuser SIMO mixed RF/FSO relay networks with opportunistic user scheduling," *IEEE Trans. Wireless Commun.*, vol. 15, no. 9, pp. 5904–5918, Sep. 2016.

[48] A. H. A. El-Malek, A. M. Salhab, S. A. Zummo, and M.-S. Alouini, "Effect of RF interference on the security-reliability tradeoff analysis of multiuser mixed RF/FSO relay networks with power allocation," *J. Lightw. Technol.*, vol. 35, no. 9, pp. 1490–1505, May 1, 2017.

[49] N. Cherif, I. Trigui, and S. Affes, "On the performance analysis of mixed multi-aperture FSO/multiuser RF relay systems with interference," in *Proc. IEEE 18th Int. Workshop Signal Process. Adv. Wireless Commun.*, Sapporo, Japan, Jul. 2017, pp. 1–5.

[50] L. Yang, M. O. Hasna, and I. S. Ansari, "Unified performance analysis for multiuser mixed η-μ and $\mathcal{M}$-distribution dual-hop RF/FSO systems," *IEEE Trans. Wireless Commun.*, vol. 65, no. 8, pp. 3601–3613, Aug. 2017.

[51] Y. F. Al-Eryani, A. M. Salhab, S. A. Zummo, and M.-S. Alouini, "Two-way multiuser mixed RF/FSO relaying: Performance analysis and power allocation," *IEEE/OSA J. Opt. Commun. Netw.*, vol. 10, no. 4, pp. 396–408, Apr. 2018.

[52] Y. F. Al-Eryani, A. M. Salhab, S. A. Zummo, and M.-S. Alouini, "Protocol design and performance analysis of multiuser mixed RF and hybrid FSO/RF relaying with buffers," *J. Opt. Commun. Netw.*, vol. 10, no. 4, pp. 309–321, Apr. 2018.

[53] A. A. AbdelNabi, F. S. Al-Qahtani, M. Shaqfeh, S. S. Ikki, and H. M. Alnuweiri, "Performance analysis of MIMO multi-hop system with TAS/MRC in Poisson field of interferers," *IEEE Trans. Commun.*, vol. 64, no. 2, pp. 525–540, Feb. 2016.

[54] J. F. Paris, "Statistical characterization of κ-μ shadowed fading," *IEEE Trans. Veh. Technol.*, vol. 63, no. 2, pp. 518–526, Feb. 2014.

[55] I. Trigui and S. Affes, "Unified analysis and optimization of D2D communications in cellular networks over fading channels," *IEEE Trans. Commun.*, vol. 67, no. 1, pp. 724–736, Jan. 2019.

[56] I. S. Gradshteyn and I. M. Ryzhik, *Table of Integrals, Series, and Products*, 5th ed. New York, NY, USA: Academic, 1994.

[57] L. Moreno-Pozas, F. J. Lopez-Martinez, J. F. Paris, and E. Martos-Naya, "The κ-μ shadowed fading model: Unifying the κ-μ and η-μ distributions," *IEEE Trans. Veh. Technol.*, vol. 65, no. 12, pp. 9630–9641, Dec. 2016.

[58] A. M. Mathai, R. K. Saxena, and H. J. Haubold, *The H-Function: Theory and Applications*. Springer Science & Business Media, 2009.

[59] I. Trigui, S. Affes, and A. Stephenne, "Closed-form error analysis of variable-gain multihop systems in Nakagami-m fading channels," *IEEE Trans. Commun.*, vol. 59, no. 8, pp. 2285–2295, Aug. 2011.

[60] P. K. Mittal and K. C. Gupta, "An integral involving generalized function of two variables," *Proc. Indian Acad. Sci. A*, vol. 75, no. 3, pp. 117–123, 1972.

[61] M. K. Simon and M.-S. Alouini, *Digital Communication Over Fading Channels*, vol. 95. Hoboken, NJ, USA: Wiley, 2005.

[62] V. A. Aalo, K. P. Peppas, G. Efthymoglou, M. M. Alwakeel, and S. S. Alwakeel, "Serial amplify-and-forward relay transmission systems in Nakagami-m fading channels with a Poisson interference field," *IEEE Trans. Veh. Technol.*, vol. 63, no. 5, pp. 2183–2196, Jun. 2014.

[63] Z. Ghassemlooy, W. Popoola, and S. Rajbhandari, *Optical Wireless Communications*. Boca Raton, FL, USA: CRC Press, 2012.

[64] Y. Azar, G. N. Wong, K. Wang, R. Mayzus, J. K. Schulz, H. Zhao, F. Gutierrez, Jr., D. Hwang, and T. S. Rappapor, "28 GHz propagation measurements for outdoor cellular communications using steerable beam antennas in New York city," in *Proc. IEEE Int. Conf. Commun. (ICC)*, Jun. 2013, pp. 5143–5147.

[65] T. S. Rappaport, F. Gutierrez, Jr., E. Ben-Dor, J. N. Murdock, Y. Qiao, and J. I. Tamir, "Broadband millimeter-wave propagation measurements and models using adaptive-beam antennas for outdoor urban cellular communications," *IEEE Trans. Antennas Propag.*, vol. 61, no. 4, pp. 1850–1859, Apr. 2013.

[66] A. Kilbas and M. Saigo, *H-Transforms: Theory and Applications*. Boca Raton, FL, USA: CRC Press, 2004.

IMÈNE TRIGUI (S'10–M'15) received the M.Sc. and Ph.D. degrees (Hons.) from the National Institute of Scientific Research (INRS-EMT), University of Quebec, Montreal, QC, Canada, in 2010 and 2015, respectively. From 2016 to 2018, she was a Postdoctoral Research Fellow with the Department of Electrical Engineering, Toronto University, Toronto, ON, Canada. Her research interests are in wireless communications and signal processing. In recognition of her academic, research, and scholarly achievements, she was a recipient of several major awards, including the Natural Sciences and Engineering Research Council of Canada (NSERC) Postdoctoral Fellowship (2016–2018), and the top-tier Alexander-Graham-Bell Canada Graduate Scholarship from the National Sciences and Engineering Research Council (2012–2014). She had to decline other Ph.D. and postdoctoral scholarships offered over the same period from the Fonds de recherche du Québec - Nature et technologies (FRQNT). She was previously a recipient of an Undergraduate Student Fellowship from the Tunisian Ministry of Communications. She also received the Best Paper Award at the IEEE VTC'2010-Fall. She serves regularly as a Reviewer for many top international journals and conferences in her field.

SOFIÈNE AFFES (S'95–SM'05) received the Diplome d'Ingénieur in telecommunications and the Ph.D. degree (Hons.) in signal processing from Télécom ParisTech (ENST), Paris, France, in 1992 and 1995, respectively. He was a Research Associate with INRS, Montreal, QC, Canada, until 1997; an Assistant Professor, until 2000; and an Associate Professor, until 2009. He is currently a Full Professor and the Director of PERWADE, a unique M4 million research-training program on wireless in Canada involving 27 partners from eight universities and ten industrial organizations. He currently serves as a member of the Editorial Board of the *MDPI Sensors Journal* and the Advisory Board of the *MDPI Multidisciplinary Journal Sci*. He has been twice a recipient of a Discovery Accelerator Supplement Award from NSERC, from 2008 to 2011 and from 2013 to 2016. From 2003 to 2013, he was the Canada Research Chair in wireless communications. Since 2017, he holds the Cyrille-Duquet Research Chair in telecommunications. In 2006, 2015, and 2017, he served as the General Co-Chair or Chair of the IEEE VTC'2006-Fall, the IEEE ICUWB'2015, and the IEEE PIMRC'2017, respectively, all held in Montreal, QC, Canada. In 2008 and 2015, he received the IEEE VTC Chair Recognition Award from the IEEE VTS and the IEEE ICUWB Chair Recognition Certificate from the IEEE MTT-S for exemplary contributions to the success of both events, respectively. He previously served as an Associate Editor for the IEEE TRANSACTIONS ON WIRELESS COMMUNICATIONS, the IEEE TRANSACTIONS ON COMMUNICATIONS, the IEEE TRANSACTIONS ON SIGNAL PROCESSING, the *Journal of Electrical and Computer Engineering* (Hindawi), and the *Journal of Wireless Communications and Mobile Computing* (Wiley).

ANAS M. SALHAB (S'11–M'14–SM'17) received the B.Sc. degree in electrical engineering from Palestine Polytechnic University, Hebron, Palestine, in 2004, the M.Sc. degree in electrical engineering from the Jordan University of Science and Technology, Irbid, Jordan, in 2007, and the Ph.D. degree from the King Fahd University of Petroleum and Minerals (KFUPM), Dhahran, Saudi Arabia, in 2013. From 2013 to 2014, he was a Postdoctoral Fellow with the Electrical Engineering Department, KFUPM. He is currently an Assistant Professor and the Assistant Director of the Science and Technology Unit with the Deanship of Scientific Research, KFUPM. His research interests span special topics in modeling and performance analysis of wireless communication systems, including cooperative relay networks, cognitive radio relay networks, free space optical networks, visible light communications, and co-channel interference. He was selected as an Exemplary Reviewer by the IEEE WIRELESS COMMUNICATIONS LETTERS for his reviewing service, in 2014. Moreover, he received the KFUPM Best Research Project Award as a Co-Investigator among the projects, in 2013 and 2014 and in 2014 and 2015, respectively.

MOHAMED-SLIM ALOUINI (S'94–M'98–SM'03–F'09) was born in Tunis, Tunisia. He received the Ph.D. degree in electrical engineering from the California Institute of Technology (Caltech), Pasadena, CA, USA, in 1998. He has served as a Faculty Member with the University of Minnesota, Minneapolis, MN, USA, and with the Texas A&M University at Qatar, Education City, Doha, Qatar, before joining the King Abdullah University of Science and Technology (KAUST), Thuwal, Saudi Arabia, as a Professor of electrical engineering, in 2009. His current research interests include the modeling, design, and performance analysis of wireless communication systems.

• • •